AD-A065 468 AIR FORCE INST OF TECH WRIGHT-PATTERSON AFB OHIO F/G 4/2
DIURNAL VARIATION OF WIND PROFILES ACROSS MOUNTAINOUS TERRAIN D--ETC(U)
1978 J A JACKSON
UNCLASSIFIED AFIT-CI-79-113T NL

| OF |
AD
A065468

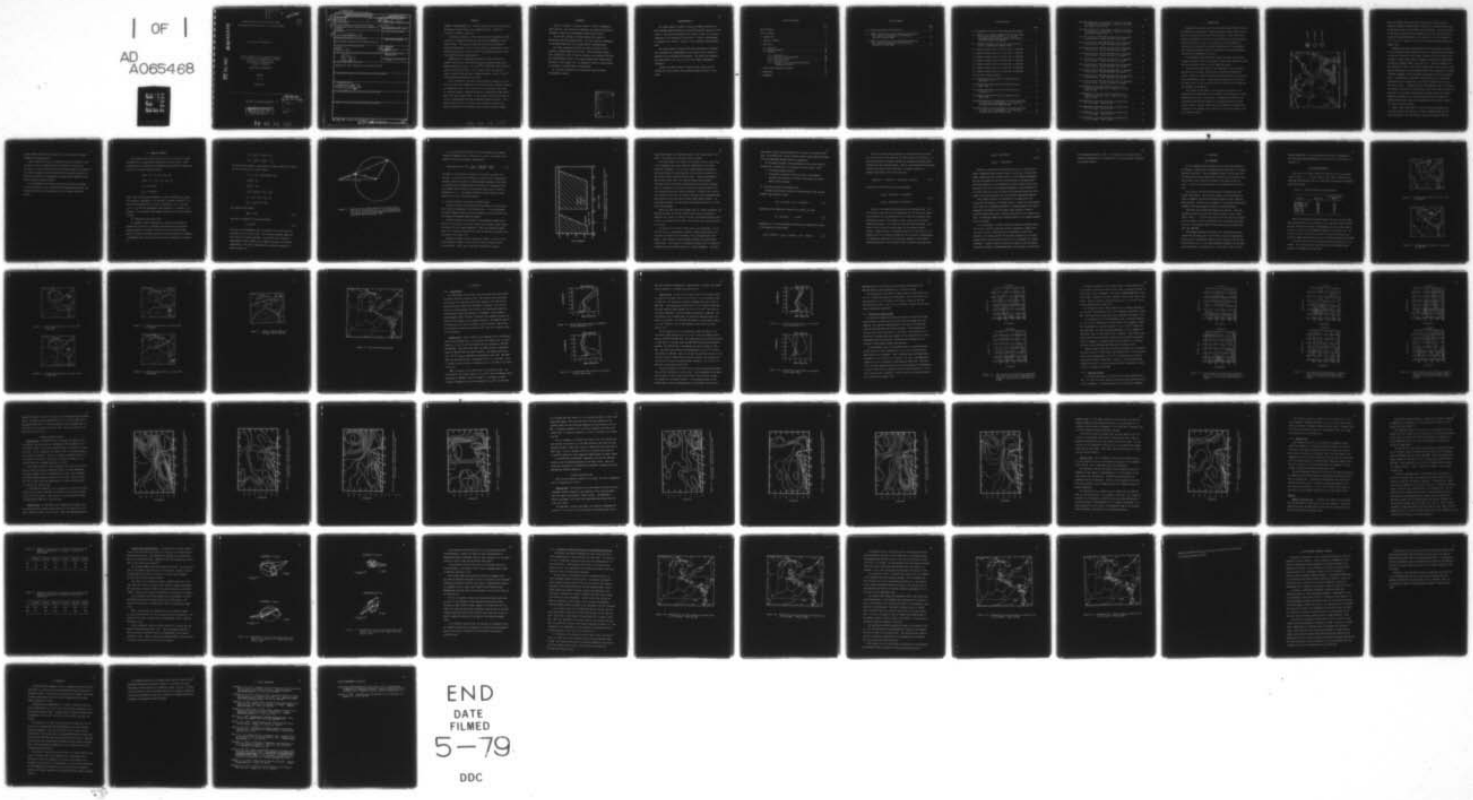

END
DATE
FILMED
5-79
DDC

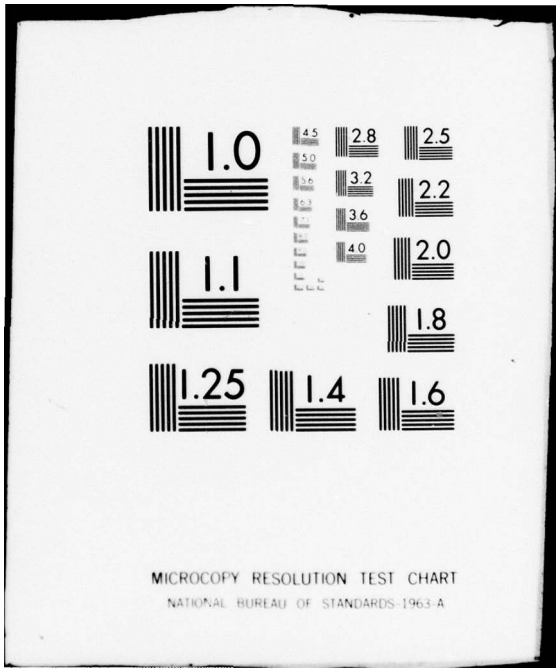
1.0
1.1
1.25
1.4
1.6
1.8
2.0
2.2
2.5
2.8
3.2
3.6
4.0
4.5
5.0
5.6
MICROCOPY RESOLUTION TEST CHART
NATIONAL BUREAU OF STANDARDS-1963-A

(1)

B.S.

DIURNAL VARIATION OF WIND PROFILES ACROSS MOUNTAINOUS TERRAIN DURING AN AIR STAGNATION PERIOD

by

JULIUS AUGUSTUS JACKSON, JR.

A thesis submitted to the Graduate Faculty of
North Carolina State University at Raleigh
in partial fulfillment of the
requirements for the Degree of
Master of Science

DEPARTMENT OF METEOROLOGY

RALEIGH

1 9 7 8

APPROVED BY:

Chairman of Advisory Committee

UNCLASSIFIED

SECURITY CLASSIFICATION OF THIS PAGE (When Data Entered)

REPORT DOCUMENTATION PAGE	READ INSTRUCTIONS BEFORE COMPLETING FORM
1. REPORT NUMBER: AFIT-CI-79-113T	2. GOVT ACCESSION NO.
	3. RECIPIENT'S CATALOG NUMBER: Master's
4. TITLE (and Subtitle): Diurnal Variation of Wind Profiles Across Mountainous Terrain during an Air Stagnation Period.	5. TYPE OF REPORT & PERIOD COVERED: Thesis
	6. PERFORMING ORG. REPORT NUMBER
7. AUTHOR(s): Julius Augustus Jackson, Jr.	8. CONTRACT OR GRANT NUMBER(s)
9. PERFORMING ORGANIZATION NAME AND ADDRESS: AFIT student at North Carolina State University	10. PROGRAM ELEMENT, PROJECT, TASK AREA & WORK UNIT NUMBERS
11. CONTROLLING OFFICE NAME AND ADDRESS: AFIT/CI, WPAFB OH 45433	12. REPORT DATE: 1978
	13. NUMBER OF PAGES: 63
14. MONITORING AGENCY NAME & ADDRESS (if different from Controlling Office): 72p.	15. SECURITY CLASS. (of this report): UNCLASSIFIED
	15a. DECLASSIFICATION/DOWNGRADING SCHEDULE

16. DISTRIBUTION STATEMENT (of this Report)

Approved for Public Release, Distribution Unlimited

17. DISTRIBUTION STATEMENT (of the abstract entered in Block 20, if different from Report)

18. SUPPLEMENTARY NOTES

JOSEPH P. HIPPS, Major, USAF
Director of Information, AFIT
FEB 8 1979

19. KEY WORDS (Continue on reverse side if necessary and identify by block number)

20. ABSTRACT (Continue on reverse side if necessary and identify by block number)

DD FORM 1 JAN 73 1473 EDITION OF 1 NOV 65 IS OBSOLETE

UNCLASSIFIED

SECURITY CLASSIFICATION OF THIS PAGE (When Data Entered)

ABSTRACT

JACKSON, JULIUS AUGUSTUS, JR. Diurnal Variation of Wind Profiles Across Mountainous Terrain During an Air Stagnation Period. (Under the direction of WALTER D. BACH, JR.)

The diurnal variation of wind profiles across mountainous terrain during an air stagnation period was evaluated for seven days in the summer of 1957. The study was conducted across the North-Central Appalachian Mountains, an area of heavy pollution concentration. The study was divided into easterly (16-18 July, 1957) and westerly (19-22 July, 1957) flow across the mountains.

Examination over the seven days showed a diurnal variation in boundary layer winds on the eastern side of the mountain range with a maximum amplitude of about 3 to 4 m sec^{-1} at 1000-1500 m MSL in both the easterly and westerly flows. On the western side of the mountain range, a diurnal variation with a maximum amplitude of about 4 m sec^{-1} at 600-1100 m MSL occurred in both flows.

This oscillation in the lower levels showed the presence of a low-level jet, which was unexpected in that this study was conducted during an air stagnation period. The low-level jet in the easterly flow across the mountains reaches a maximum wind speed at approximately 0600 GMT at about 300 m above ground level. In the westerly flow, the low-level jet occurs at approximately 1200 GMT at 600-800 m above the ground. This low-level jet is due to an inertial type oscillation driven by the diurnal variation of the frictional forces aided by thermal forcing.

BIOGRAPHY

Julius A. Jackson, Jr. was born August 9, 1941, in Washington, North Carolina. He received his elementary and secondary education in Washington, graduating from Washington High School in 1959.

He received a Bachelor of Science degree with a major in Meteorology from Texas A&M University. He also received a commission in the United States Air Force through Officer Training School.

The author entered the Air Force in 1959, and served in the capacity of Weather Observer until 1969. After receiving a degree and a commission in 1971, he has held positions as a Weather Forecaster and a Staff Weather Officer. The author entered North Carolina State University in the spring, 1977, to undertake a course of study leading to the Master of Science degree in Meteorology.

Mr. Jackson is married to the former Miss Linda Gayle Knox of Montgomery, Alabama.

ACKNOWLEDGMENTS

The author wishes to thank the Research Triangle Institute and North Carolina State University for providing financial support for this project. The advice and guidance of Dr. Walter D. Bach, Jr. have been invaluable in the completion of this study. A special acknowledgment is extended to Dr. Walter J. Saucier for his assistance and encouragement.

The author wishes to thank the Air Force Institute of Technology which permitted the accomplishment of this study, and Dr. Charles E. Anderson for his knowledge and assistance. The author also expresses his appreciation to Dr. Ted L. Tsui for his computer programming assistance.

Finally, the author wishes to thank his wife, Linda, and his children for their patience and sacrifice during the course of this study.

TABLE OF CONTENTS

LIST OF TABLES

LIST OF FIGURES

1. INTRODUCTION

Stagnating anticyclones are often associated with incidents of heavy air pollution in urban areas. These anticyclones usually linger over an area for a protracted period (four days or more). During this period, surface wind speeds may be very low, and visibility and vertical mixing are often restricted. Thus, the circulation is often thought to be insufficient to disperse the accumulated pollutants of the atmosphere. The resulting accumulation may cause distressful and possibly hazardous conditions for inhabitants of the area.

The stagnating anticyclones that produce the major air pollution episodes are usually found in the eastern United States (Korshover, 1975), and are most likely to occur in late summer and autumn.

The northeast United States is very susceptable to air pollution episodes due to the heavy concentration of industry and population centers. Figure 1.1 shows the annual SO_2 emission density in the northeast and Ohio Valley areas. These pollution episodes not only affect the urban areas, but the non-urban areas are affected due to dispersion and transport of pollutants.

The purpose of this study is to investigate the effects of the mountains on the wind profile in the boundary layer during an air stagnation period, as well as the effects of boundary layer winds on air pollution dispersion and transport in a stagnation period over mountainous terrain. Various studies have been completed on diurnal wind variation in the boundary layer, but not any (as could be found) in an air stagnation period.

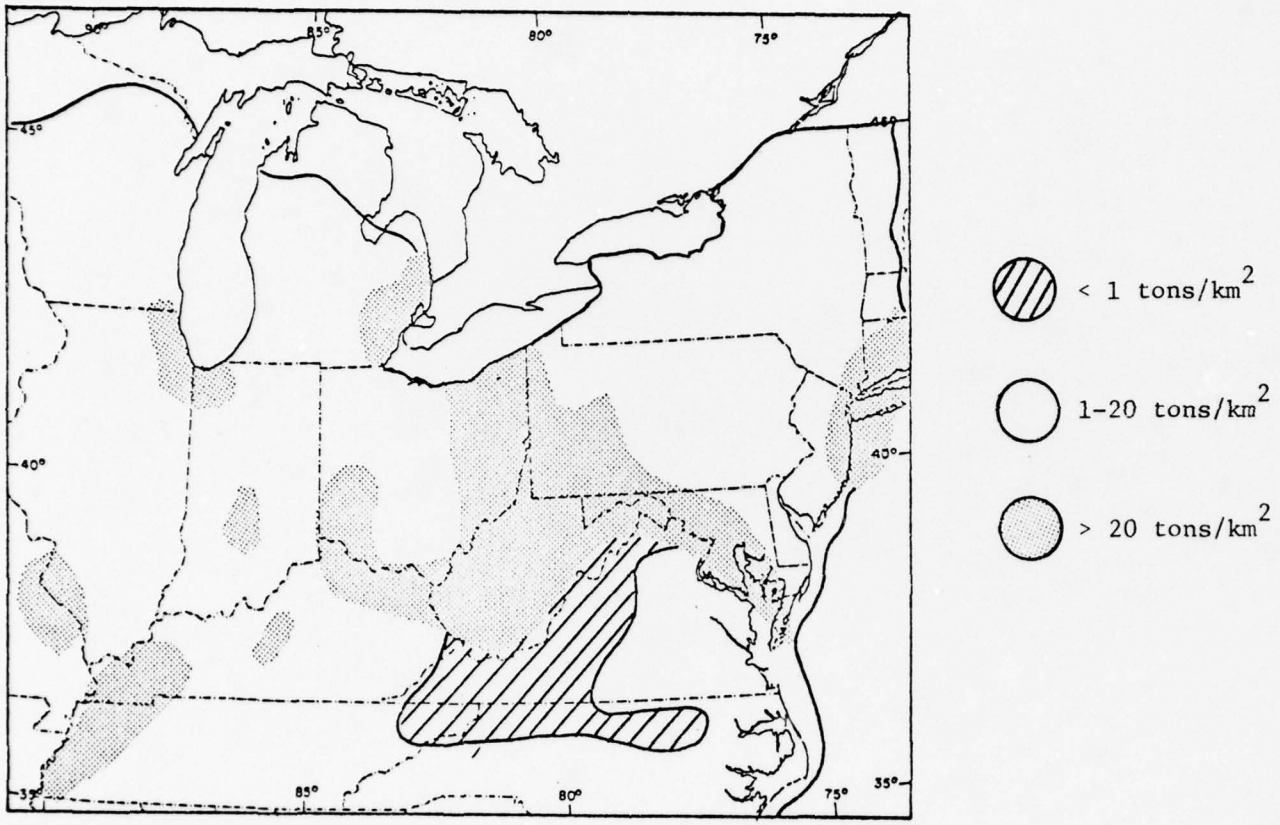

Figure 1.1. Geographic variation in annual SO_2 emission density (after EPA report 450/2-75-007).

Bonner and Paegle (1970) found that boundary layer winds oscillate diurnally reaching a maximum speed at night and a minimum during the day at elevations between 50 and 2000 m above the ground. The wind variation is especially pronounced with southerly flow over the central plains to the east of the Rocky Mountains. The amplitude of this oscillation is 2 to 3 m sec^{-1} at levels of 0.5 and 2.0 km above the ground (Hering and Borden, 1967).

Boundary layer wind oscillation may arise from periodic variation in the horizontal pressure gradient force as in mountain wind circulation or they may be driven by day-to-night variation in the frictional force. A number of theories have been put forward to explain this diurnal wind oscillation (commonly termed "low-level jet"). The most pervasive has been Blackadar's (1957), that the jet results from a free inertial oscillation superimposed on the geostrophic basic flow, initiated by the rapid nocturnal breakdown of the frictional restraining force in the boundary layer. The mechanism is grounded in the diurnal cycle of insolation, which gives rise to variations in the vertical temperature lapse rate and eddy viscosity. Attempts (Buajitti and Blackadar, 1957) to simulate the behavior indicated that both the mean value of the eddy viscosity and amplitude of its diurnal variations must decrease rapidly with height. Numerical experiments with constant geostrophic wind and diurnally varying eddy viscosity duplicate reasonable well the observed oscillation over the central plains.

Wexler (1961) stated that it is not the local radiational and frictional effects that produce the level of maximum winds, but the bulk properties of the flow caused by large scale inertial effects.

Holton (1967) attributed the low-level jet to the effects of diurnal heating over sloping terrain.

Lettau (1967) stated that the Blackadar and Wexler theories on the low-level jet may be summarized with the addition of a new theory. The theory is that the model of thermo-tidal winds require the presence of of a large to mesoscale terrain slope with the additional feature of a definite statistical or thermodynamic coupling between large-scale barometric fields and terrain contours.

It is attempted in this study to describe the diurnal variations of the wind profile across the North-Central Appalachian Mountains, and to find what effects the mountains have on the boundary layer wind profile.

2. TECHNICAL APPROACH

The boundary layer wind oscillation occurs as a result of varying influences of the accelerations experienced by an air parcel. These accelerations are expressed by the Navier-Stokes equations of horizontal motion in a rotating coordinate system:

$$du/dt = fv - fv_g + F_x = fv_a + F_x$$

$$dv/dt = -fu + fu_g + F_y = -fu_a + F_y$$

$$fv_g = (1/\rho)\partial p/\partial x$$

$$fu_g = -(1/\rho)\partial p/\partial y$$

where u and v are velocity components in x and y directions, u_g and v_g are geostrophic components, f is the coriolis parameter ($2\Omega\sin\phi$), F is the friction component in the x and y directions, u_a (= $u - u_g$) and v_a (= $v - v_g$) are the ageostrophic wind components, ρ is density, p is pressure, Ω is the earth's axial angular velocity, and ϕ is the latitude on earth.

a). Horizontal frictionless flow

In Blackadar's (1957) explanation of inertial oscillation, he assumed that the motion is completely horizontal and the horizontal pressure gradient is constant in time and in each horizontal plane. Above the nocturnal inversion, where vertical eddy transport of momentum is negligible and F_x and F_y may be assumed zero, Equation (1.1) reduces to:

$$d(u - u_g)/dt = du_a/dt = fv_a$$

$$d(v - v_g)/dt = dv_a/dt = -fu_a$$

The solution and geometric interpretation of these equations are facilitated by introducing the complex number:

$$W = u_a + iv_a = \text{ageostrophic wind}$$

$$du_a/dt = fv_a$$

$$dv_a/dt = -fu_a$$

$$d(u_a + iv_a)/dt = f(v_a - iu_a)$$

$$W.i = iu_a + i^2v_a = iu_a - v_a$$

$$d(u_a + iv_a)/dt = f(-iW)$$

The equation then becomes,

$$dW/dt = -ifW \tag{1.2}$$

which may be integrated to give the solution,

$$W = W_o e^{-ift} \tag{1.3}$$

where W_o is the ageostrophic wind (or deviation of the wind from the geostrophic) at the initial time. This equation expresses simple harmonic motion of constant amplitude. The initial time is chosen as approximately sunset, because this is where frictional forces become insignificant. The type of motion which the solution represents is shown in Figure 2.1.

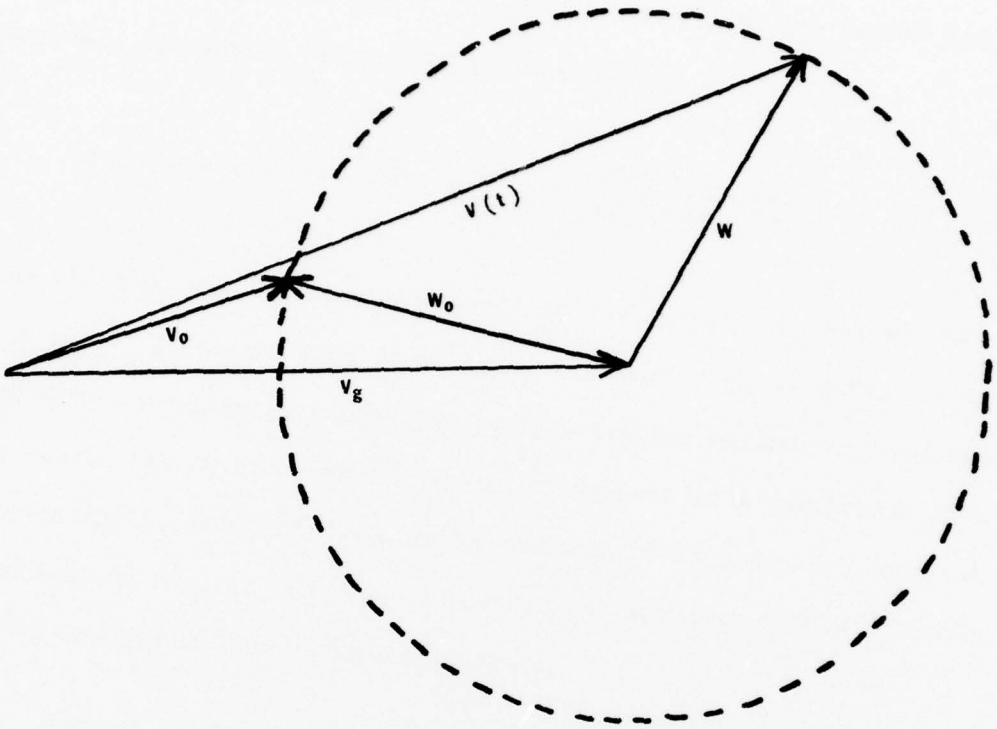

Figure 2.1. Relation of the complex number W and the wind vector V(t) to the initial values W_o, V_o, and the geostrophic wind vector V_g during a frictionally initiated inertial oscillation (after Blackadar, 1957).

It is seen that the deviation from the geostrophic wind remains constant in magnitude, but it rotates to the right, its period for one complete revolution being half a pendulum day.

$$\tfrac{1}{2}\text{PD(pendulum day)} = \frac{2\pi}{f} = \frac{2\pi}{2\Omega\sin\phi} = \frac{2\pi(24\text{ hr})}{2(2\pi)\sin\phi} = \frac{12\text{ hr}}{\sin\phi} \qquad (1.4)$$

The phase of the oscillation depends on the phase of W_o and on the latitude. It can be seen from Figure 2.1 that if W_o is a typical geostrophic deviation at sunset, a supergeostrophic maximum of wind speed is reached about six pendulum hours or one-half of a revolution later (for example, about 12 hours at San Antonio, Texas, and 9.5 hours at Washington, D. C.). The assumed conditions are most likely to occur above the top of the nocturnal inversion.

b). Diurnal variation of friction in boundary layer

Friction reduces the wind speed near the surface of the earth and thus reduces the magnitude of the coriolis force. It also dissipates horizontal momentum causing a vertical gradient in the wind profile and the transfer of momentum toward the ground.

The layer adjacent to the surface is the momentum boundary layer. The top of this layer is the level at which the turbulent mixing induced by surface friction becomes negligible. Above that momentum boundary layer is the inertial boundary layer, where the motion is horizontal and frictionless (see Figure 2.2).

During the daytime, surface heating and transfer of heat into the lower atmosphere produces a deep layer with nearly adiabetic lapse rate conditions. Under these conditions momentum may be freely

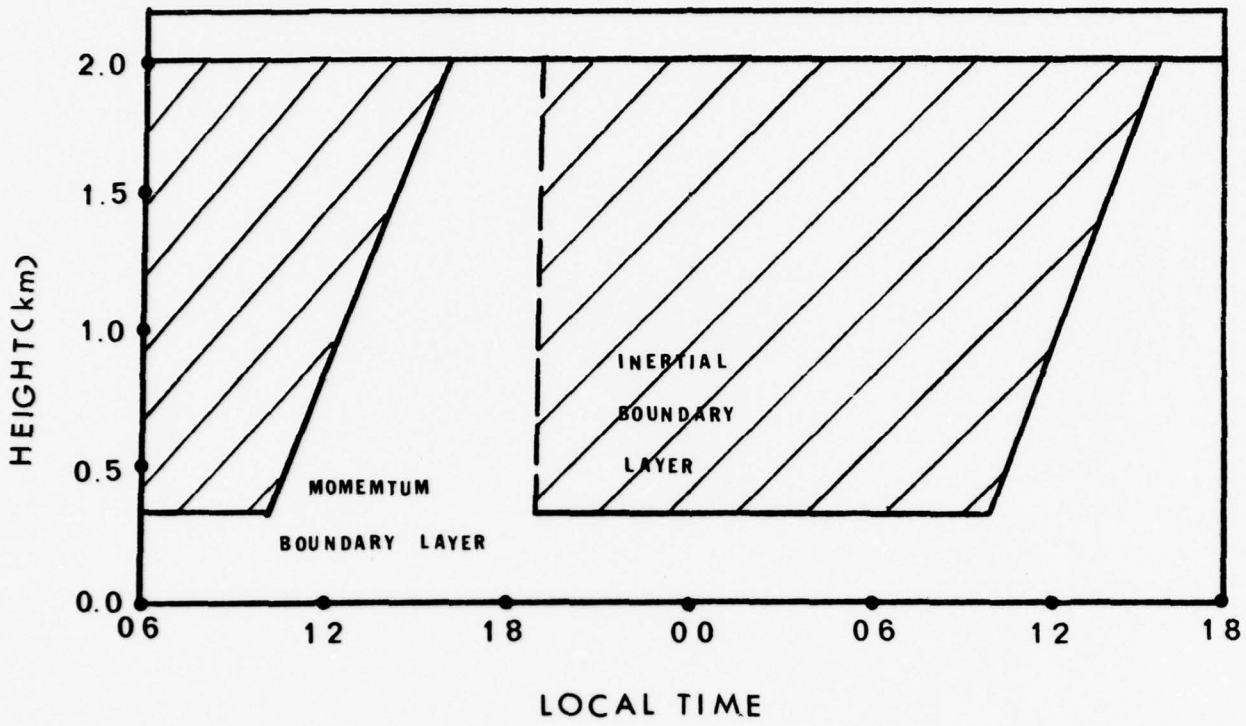

Figure 2.2. Schematic diagram of the diurnal variation in the depth of the momentum boundary layer (after Hoxit, 1973).

transferred downward. The momentum boundary layer becomes nearly 2 km thick. Frictional forces are large near the ground.

Just after sunset, the surface cools rapidly, and the lowest layer of the atmosphere cools also, while the temperatures above remain essentially unchanged. The low level cooling suppresses mechanical and buoyant mixing by stabilizing the air and leads to formation of a new and much thinner momentum boundary layer. Above the developing ground based stable layer, the turbulent mixing ceases rapidly. Frictional forces aloft become insignificant and an inertial boundary layer is established. The inertial oscillation develops rapidly with the dissipation mechanism largely eliminated. Eventually the coriolis force becomes greater than the pressure gradient force; supergeostrophic winds develop as the wind vector rotates toward higher pressure. In the middle latitudes, the wind speeds reach maximum values one to three hours after midnight.

During the night and early morning hours in a stable atmosphere, the physical processes in the 300 to 1500 m layer above the ground are apparently not related to surface friction. The momentum boundary layer is only a few hundred meters thick. The inertial layer develops shortly after sunset.

By sunrise, the low level stable layer is well developed. In the inertial layer, an ageostrophic component towards higher pressure has developed in response to the formation of the supergeostrophic wind speeds. After sunrise, surface heating eliminates the ground based surface layer. The mixing in the momentum boundary layer is enhanced by eliminating the restraining effects of a stable atmosphere. The upper

wind speeds decrease through deepening of the layer of frictional influence. By mid-afternoon, as the turbulent mixing reaches higher and higher, the layer exhibiting inertial motion is eliminated.

In the middle latitudes, the wind maximum in the inertial layer is destroyed by a combination of two separate processes (Hoxit, 1973):

1. flow towards higher pressure
2. dissipation by turbulent scale processes as the momentum boundary layer replaces the inertial layer during the period 0900 to 1500 local time.

c). Diurnal variation in geostrophic wind.

To express the diurnal variation in the geostrophic wind, the geostrophic wind equation is used:

$$fv_g = (1/\rho)\partial p/\partial x \ , \ fu_g = -(1/\rho)\partial p/\partial y \qquad (1.5)$$

together with the hydrostatic equation and equation of state:

$$g = -(1/\rho)\partial p/\partial z \ , \ \rho = p/RT \qquad (1.6)$$

Elimination of ρ in the geostrophic and hydrostatic expression by means of the equation of state yields:

$$fv_g/T = R\partial \ln p/\partial x \ , \ fu_g/T = -R\partial \ln p/\partial y \ , \ g/T = -R\partial \ln p/\partial z \qquad (1.7)$$

The first of these three equations are differentiated with respect to z, and the last of the equations are differentiated with respect to x, with the derivative of pressure between the resulting expressions being eliminated by cross-differentiation. Then by cross-differentiating between between the second and third equations to eliminate reference to pressure again (Hess, 1959), the results are:

$$\partial(fv_g/T)/\partial z = -\partial(g/T)/\partial x \ , \ \partial(fu_g/T)/\partial z = \partial(g/T)/\partial y \tag{1.8}$$

completing the differentiation and rearrangement

$$\partial v_g/\partial z = (g/fT)\partial T/\partial x + (v_g/T)\partial T/\partial z$$

$$\partial u_g/\partial z = -(g/fT)\partial T/\partial y + (u_g/T)\partial T/\partial z \tag{1.9}$$

These are the thermal wind equations in differentiated form. The first terms on the right are the contributions by the horizontal temperature gradient, and the second terms on the right are correction terms involving the slope of the isobaric surface (u_g, v_g) and the vertical temperature gradient. The correction terms are relatively small. They vanish if the xy plane is placed tangent to the pressure surface locally. Since the slope of a pressure surface is of the order of 1 in 10,000, there is no practical distinction in the accuracy of determining the temperature gradients in the horizontal compared to the constant pressure perspective. We may neglect those correction terms and write:

$$\partial v_g/\partial z = (g/fT)\,\partial T/\partial x$$

$$\partial u_g/\partial z = -(g/fT)\,\partial T/\partial y \qquad (1.10)$$

Therefore, equation (1.10) requires that for v_g to increase with height, temperatures must increase along x, and for u_g to increase with height, temperatures must decrease along y, in the Northern Hemisphere. This may be restated as the vector vertical shear of the geostrophic wind lying parallel to the isotherms in the level surface with low temperatures on the left in the Northern Hemisphere. These properties of the thermal wind may be used to show the relationship between the vector change of wind with elevation and the horizontal temperature gradient.

These thermal effects can contribute to the amplitude of the diurnal wind oscillation over sloping terrain. Because the gravitational force vector has a component parallel to a sloping boundary, the diurnal temperature oscillation in the boundary layer provides a source of potential energy which drives a diurnal oscillation in the boundary layer wind. The momentum (Ekman layer) boundary layer and the thermal boundary layer are coupled.

If the atmosphere is stably stratified, downslope (upslope) motion will create a positive (negative) potential temperature anomaly which will in turn create a buoyancy force in opposition to the motion. Therefore, over sloping terrain the east-west component of the diurnal boundary layer wind oscillation will tend to be suppressed in a stable atmosphere. Positive stability reduces the height of the oscillation, decreases the height of maximum amplitude, and increases the ellipticity

of the hodographs (Holton, 1967). This indicates that thermal effects contribute substantially to the amplitude of the diurnal wind oscillation over sloping terrain.

3. CASE STUDY

3.1 Selection

The air stagnation period analyzed in this study was identified by Korshover, "Climatology of Stagnating Anticyclones East of the Rocky Mountains, 1936-1975." The air stagnation period of 16-22 July, 1957, was selected for analysis from general potential cases because it provided easterly flow, followed by westerly flow across the area of study. It was also selected because of the availability of the wind data.

This analysis was based on seven days of radiosonde and pilot-balloon observations. All wind data utilized in this study were obtained on magnetic tape from the National Climatic Center, Asheville, North Carolina. The data are the products of the routine observational programs of the meteorological services of the United States.

These data were obtained from Winds Aloft deck 535. This deck contains wind data for the surface and for heights of 150 m, 500 m, 1000 m, 1500 m ... The first two levels (150 m and 300 m) are heights above the surface, while the remaining levels are heights above mean sea level. The standard times for the observations were 0000, 0600, 1200, and 1800 GMT.

This stagnation period was brought on by a slowly moving anticyclone over the study area. On the 16th of July, the high pressure center was over southeastern Ontario, and by the 22nd it was off the North Carolina coast. As the high progressed southward, the flow went from northeasterly to southeasterly. On the 19th of July, the flow

became southwesterly. As the high progressed further southeastward, the flow became west-northwesterly by the 22nd of July (see Figures 3.1 through 3.7).

3.2 Analysis Approach

Wind data in the height format were analyzed for the six stations listed in Table 1.1. Of the six stations, PIT, DCA, and FNT were from radiosonde observations, while the other three stations were observations from pilot balloons.

Table 1.1. Station identifiers and elevations.

Station	Identifier	Elevations above MSL(m)
Washington, D. C.	DCA	20
Harrisburg, Pa.	HAR	107
Pittsburgh, Pa.	PIT	373
Akron, Oh.	AKN	377
Toledo, Oh.	TOL	211
Flint, Mich.	FNT	233

These six stations were selected because they are in an area where heavy concentrations of air pollutants occur, especially sulfur dioxide, and also because the stations are approximately on a line drawn perpendicular to the axis of the Appalachian Mountains (see Figure 3.8). The terrain elevations (above mean sea level) in this profile across the mountains ranged from 20 meters at DCA to 1040 meters between PIT and HAR.

The first nine levels of the observations were analyzed (up to 3.0 km MSL). The two levels (150 m and 300 m), which were heights above ground, were changed to mean sea level.

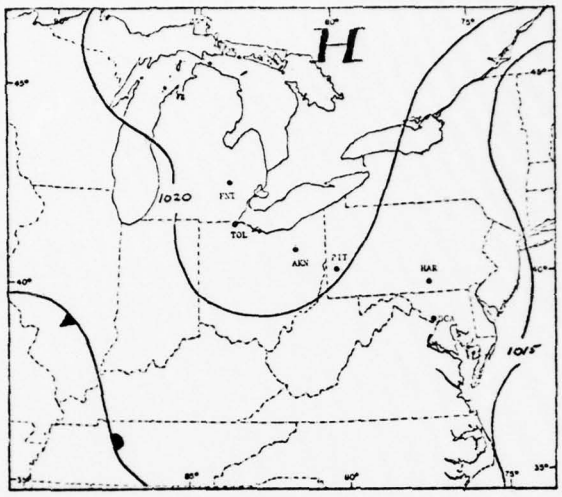

Figure 3.1. Synoptic weather chart of 16 July, 1957 at 1200 GMT.

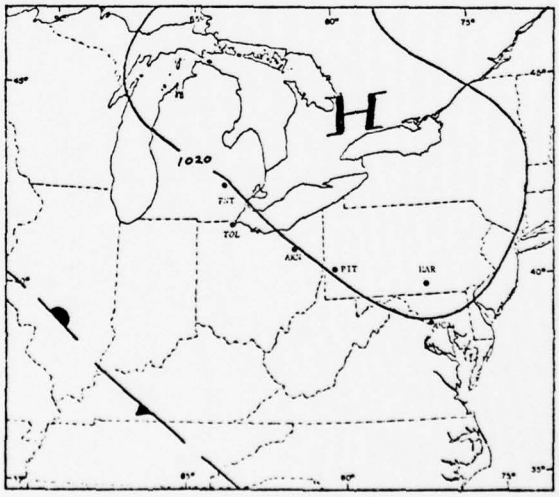

Figure 3.2. Synoptic weather chart of 17 July, 1957 at 1200 GMT.

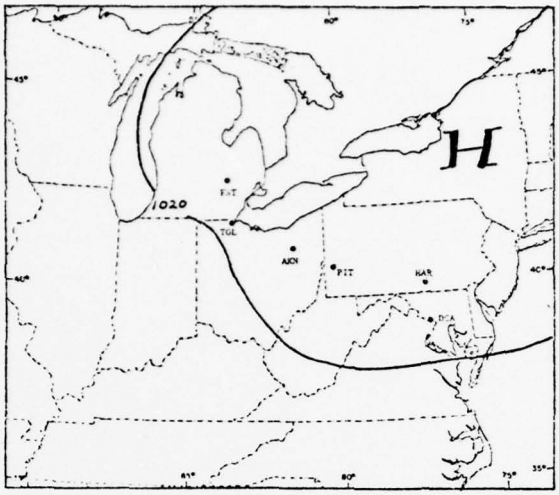

Figure 3.3. Synoptic weather chart of 18 July, 1957 at 1200 GMT.

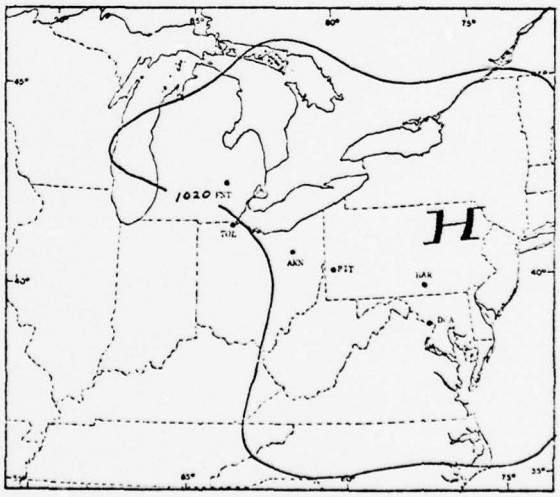

Figure 3.4. Synoptic weather chart of 19 July, 1957 at 1200 GMT.

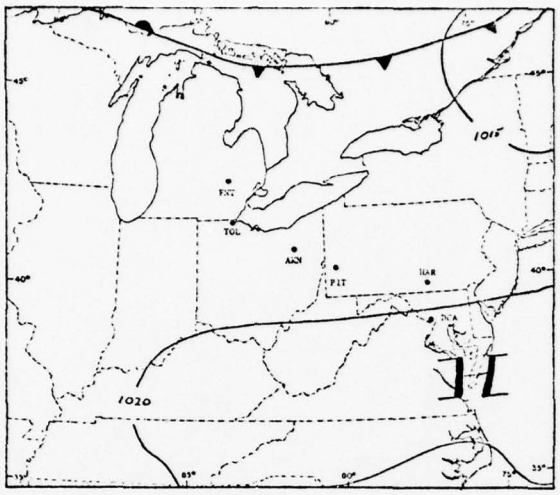

Figure 3.5. Synoptic weather chart of 20 July, 1957 at 1200 GMT.

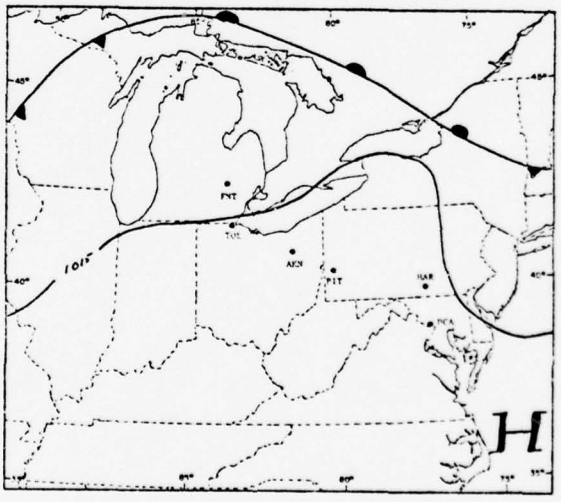

Figure 3.6. Synoptic weather chart of 21 July, 1957 at 1200 GMT.

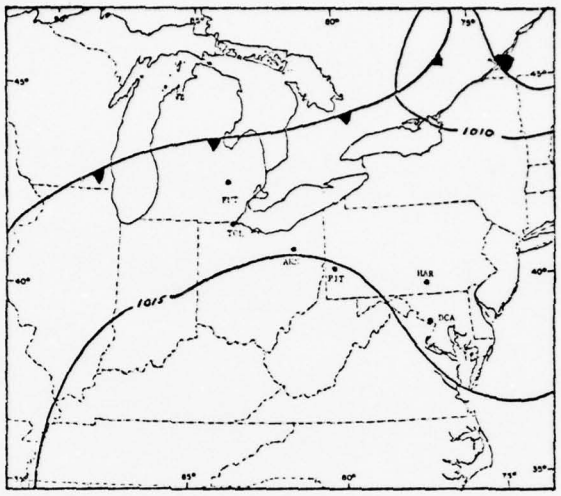

Figure 3.7. Synoptic weather chart of 22 July, 1957 at 1200 GMT.

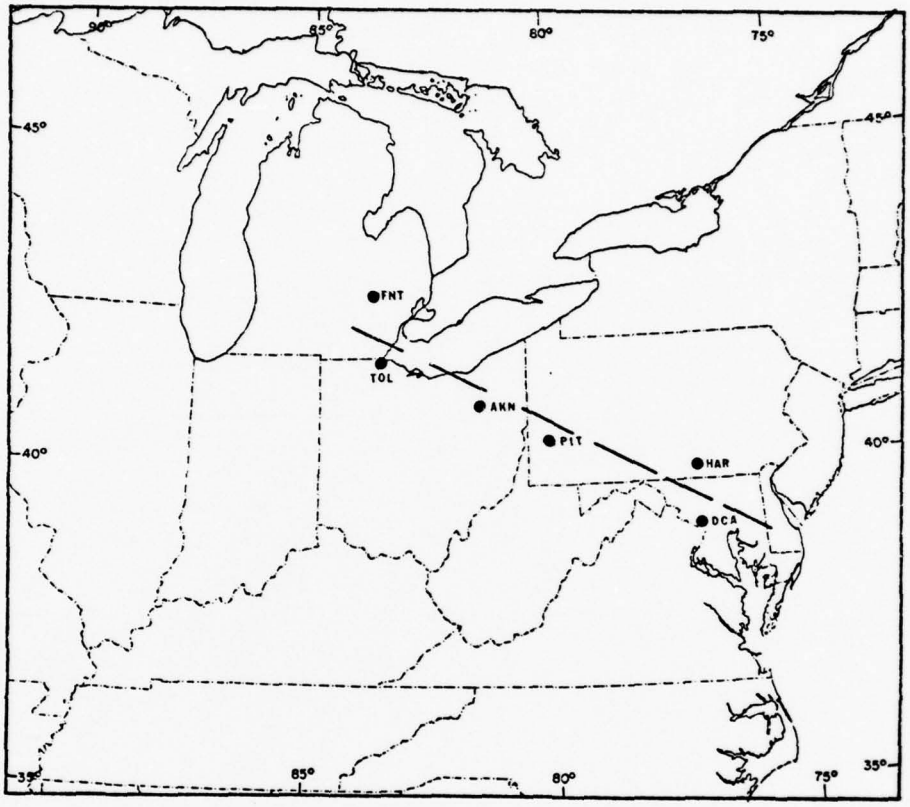

Figure 3.8. Area and stations analyzed.

3.3 Analysis

3.3.1. Wind Profile

The wind profile over the seven days was divided into two periods: an easterly flow and a westerly flow. The easterly flow as described in the study is a three-day (16-18 July) average of the wind profile. The wind direction ranged from northeast to southeast. The westerly flow is a four-day average (19-22 July) of the wind profile where the wind direction ranged from southwest to northwest. These profiles were averaged because the study is during an air stagnation period, and there is little change in the synoptic situation. The magnitude and not the direction of the wind is analyzed in these profiles. AKN and DCA were selected as stations for analysis since they are on opposite sides of the mountains.

Easterly flow. DCA is located on the windward side of the mountain range in the easterly flow. At the surface (see Figure 3.9), the winds range 2 to 3 m sec^{-1}, with the maximum velocity occurring at 1800 GMT and 0600 GMT. From 200 to 700 m MSL, the winds increase in magnitude, except at 1800 GMT when the speed decreases. The maximum wind speed (6.5 m sec^{-1}) occurs at 0600 GMT at approximately 300 m MSL. The 0000, 0600, and 1200 GMT decrease in magnitude from 1.0 to 1.5 km MSL. Above 1.5 km MSL the wind increases in magnitude up to 3.0 km MSL at all times of the day.

AKN is situated on the leeward side of the mountain range. The wind speeds at the surface range 2 to 5 m sec^{-1}, with the highest surface wind speed at 1800 GMT. From 0.5 km MSL to 1.2 km MSL, the winds increase in magnitude with the wind maxima (9.5 m sec^{-1}) at 0600 GMT.

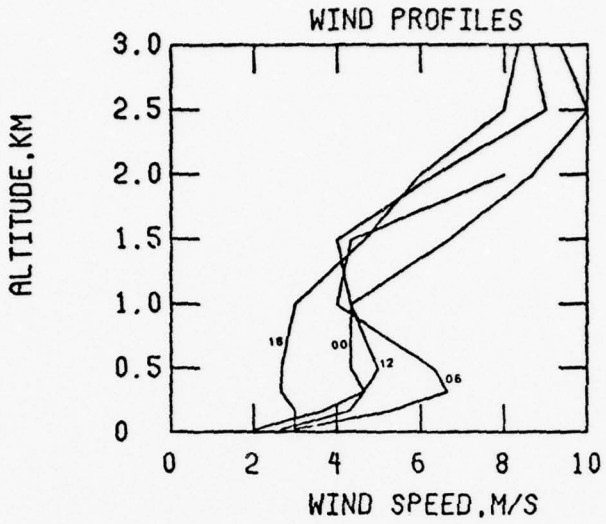

Figure 3.9. Average wind speed profile for easterly flow at Washington, D. C.

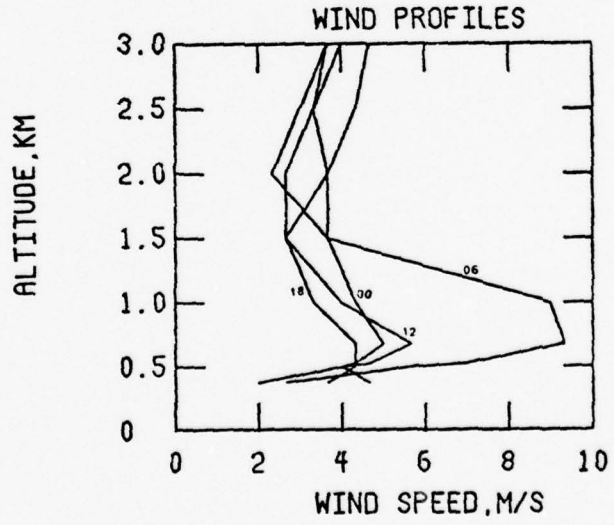

Figure 3.10. Average wind speed profile for easterly flow at Akron, Ohio.

The wind decreases in magnitude at approximately 1.5 km MSL, and remains fairly constant to 3.0 km MSL (see Figure 3.10).

Westerly flow. At DCA, on the leeward side of the mountain range, the surface flow ranged from 1.8 to 3.9 m sec^{-1}, with the highest speed at 0600 GMT. The wind profile reached a maximum wind speed at 200 to 600 m MSL. The maximum wind velocity (8 m sec^{-1}) occurred at 0600 GMT. The other profiles showed maxima, but 3.0 to 3.5 m sec^{-1} less than the profiles at 0600 GMT. The wind maximum was smallest at 1800 GMT. All the profiles show a minimum above 1.0 km MSL and remained fairly constant to 3.0 km MSL. The 0600 GMT wind profile in the westerly flow is 1.5 m sec^{-1} greater than the wind maximum in the eastern flow (see Figure 3.11).

On the windward side of the mountains at AKN (see Figure 3.12), the surface winds ranged from 2 to 3 m sec^{-1}, with the maximum surface winds at 1200 GMT and 1800 GMT. The maximum wind in the profile occurred at 1200 GMT at 1.5 km MSL, while the 0600 GMT profile had the smallest maximum. The 1200 GMT had a deep maximum of winds from 800 to 1500 m MSL. The other three profiles were approximately 4 m sec^{-1} less than the profile at 1200 GMT. Above 1.5 km MSL, the profiles were not as constant as the DCA or AKN easterly flow wind profiles.. The profiles for the FNT and TOL stations showed secondary maximum of 7 to 8 m sec^{-1} at 0600 GMT at approximately 500 m MSL.

The wind maximum in the lower levels in both the easterly and westerly profiles identifies a low-level jet. The wind maximum at the upper levels (above 1.5 km) at DCA in the easterly flow is due to an upper air trough over the western Atlantic. An interesting aspect in the surface wind is that the maximum speed in the easterly flow occurs at

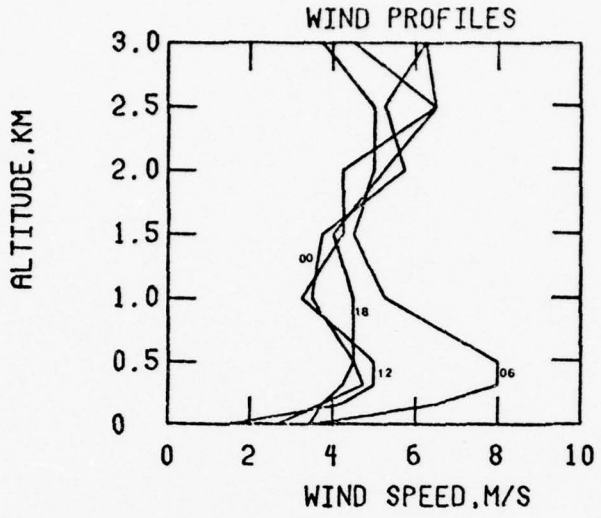

Figure 3.11. Average wind speed profile for westerly flow at Washington, D. C.

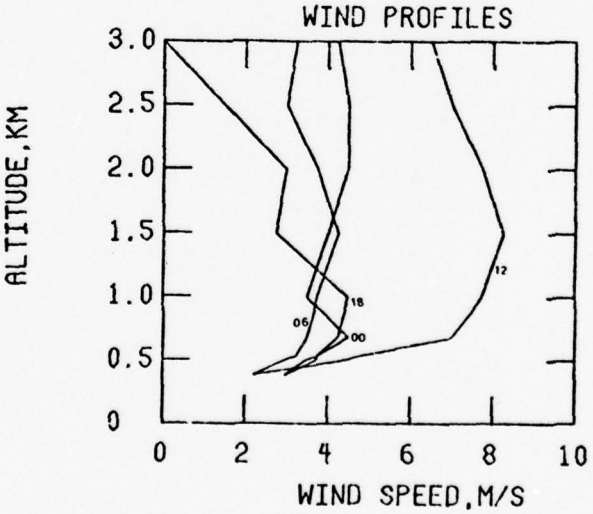

Figure 3.12. Average wind speed profile for westerly flow at Akron, Ohio.

0600 GMT while in the westerly flow the maximum surface wind is at 1800 GMT (which is more reasonable due to daytime heating).

The wind profiles also depict a sharp decrease in wind speed at the 1.0 to 1.4 km MSL level above the wind maxima. All of the profiles are fairly uniform up to 3.0 km MSL in this respect, except for the AKN 1200 GMT westerly flow. This 1.0 to 1.5 km level is where the wind flow becomes essentially geostrophic.

3.3.2 Variation in Observed Wind

To show more vividly the diurnal oscillation of wind in this stagnation period, the deviations of the wind from its average value were computed. Two stations representative of both sides of the mountain range (DCA and AKN) were selected for analysis. Levels examined are the nine levels from the surface to 3.0 km MSL. The deviation of the wind from its average value was computed for the particular day at each observation time for each level. Deviations were averaged over all the days in each series (easterly and westerly).

In the easterly flow, on the windward side of the mountain range, at DCA, there is a daily variation of 3 to 4 m sec^{-1} between 300 and 1000 m MSL in the U component. The V component shows the maximum daily variation of 2 to 3 m sec^{-1} at 1.0 km MSL. The level of maximum amplitudeiin the U and V components is approximately 1200 m MSL. Above this level, the wind changes direction, and a daily variation of approximately 4 m sec^{-1} occurs in the U component, while a daily variation of 1 to 2 m sec^{-1} occurs in the V component. There is very little diurnal variation at the surface (see Figure 3.13).

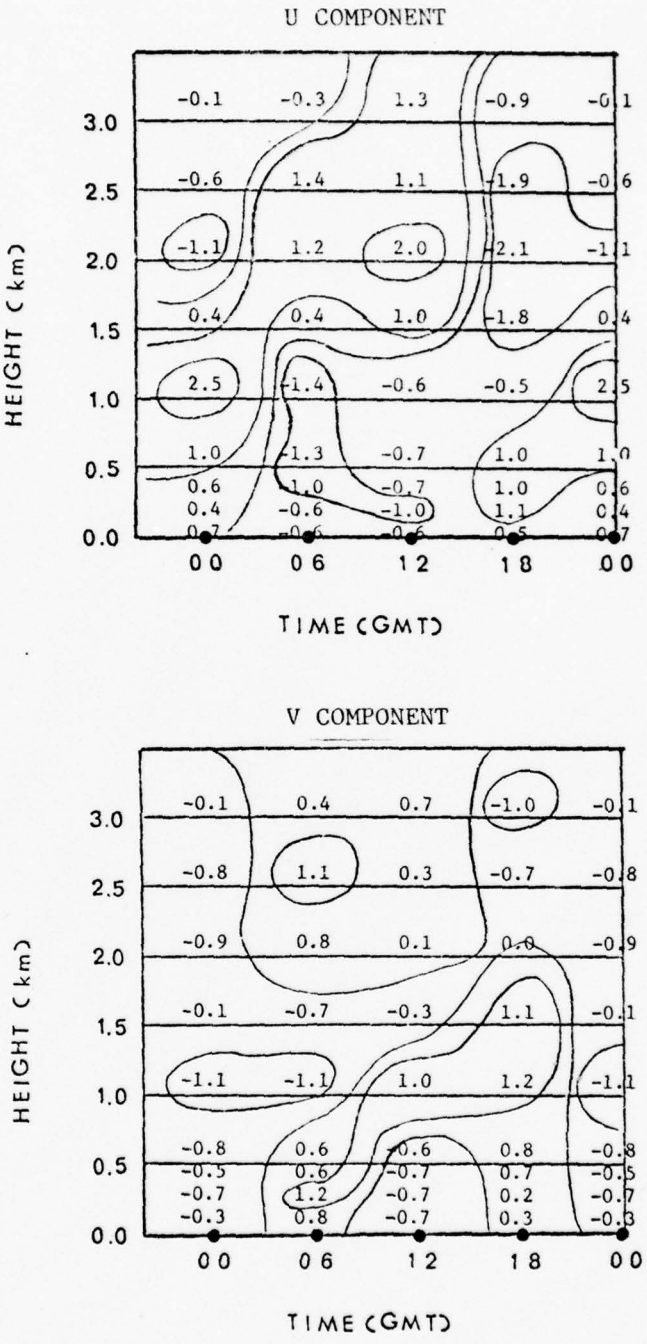

Figure 3.13. Time variation of the deviation in easterly wind from its daily mean at Washington, D. C. Values are in meters per second; times are in GMT.

At DCA in the westerly flow (leeward side), a diurnal variation of 2 to 3 m sec^{-1} occurs in the lower levels, while a variation of about 5 m sec^{-1} occurs in the V component. The level of maximum amplitude is 500 to 600 m MSL. Between 1.0 km and 2.0 km MSL, there is very little oscillation. Above 2.0 km MSL, a diurnal variation of 3 to 4 m sec^{-1} occurs in both components (see Figure 3.14).

In the easterly flow at AKN (leeward side), a diurnal variation of 4 to 6 m sec^{-1} was observed in the U and V components from 800 to 1200 m MSL. Above this level, there was little oscillation (see Figure 3.15).

In the westerly flow at AKN (windward side), the diurnal variation is 6 to 7 m sec^{-1} between 800 and 1500 m MSL in the U component, while the V component has a diurnal variation of 3 to 4 m sec^{-1} between 500 and 1000 m MSL. The level of maximum amplitude in the U component is 1600 m MSL, while it 1100 m MSL in the V component. Above these levels there is very little oscillation except for the 1200 GMT observations in the V component. The wind changes from a southwest to a northwest direction at the 1200 GMT 1000 m MSL level (see Figure 3.16).

Observed winds at DCA show a diurnal oscillation with an amplitude of nearly 3 m sec^{-1} at 1000 m MSL in the easterly flow. In the westerly flow at DCA, am amplitude of 4 m sec^{-1} is depicted with the diurnal oscillation at 1000 to 1500 m MSL. At AKN, in both the eastern and western flow there is a diurnal oscillation with a magnitude of nearly 4 m sec^{-1} from 600 to 1100 m MSL.

3.3.3. Flow Over Terrain

An analysis was made of the flow over the terrain between DCA to FNT. All nine levels were analyzed and the wind was projected into its U and V components. A study was made also of the U and V components

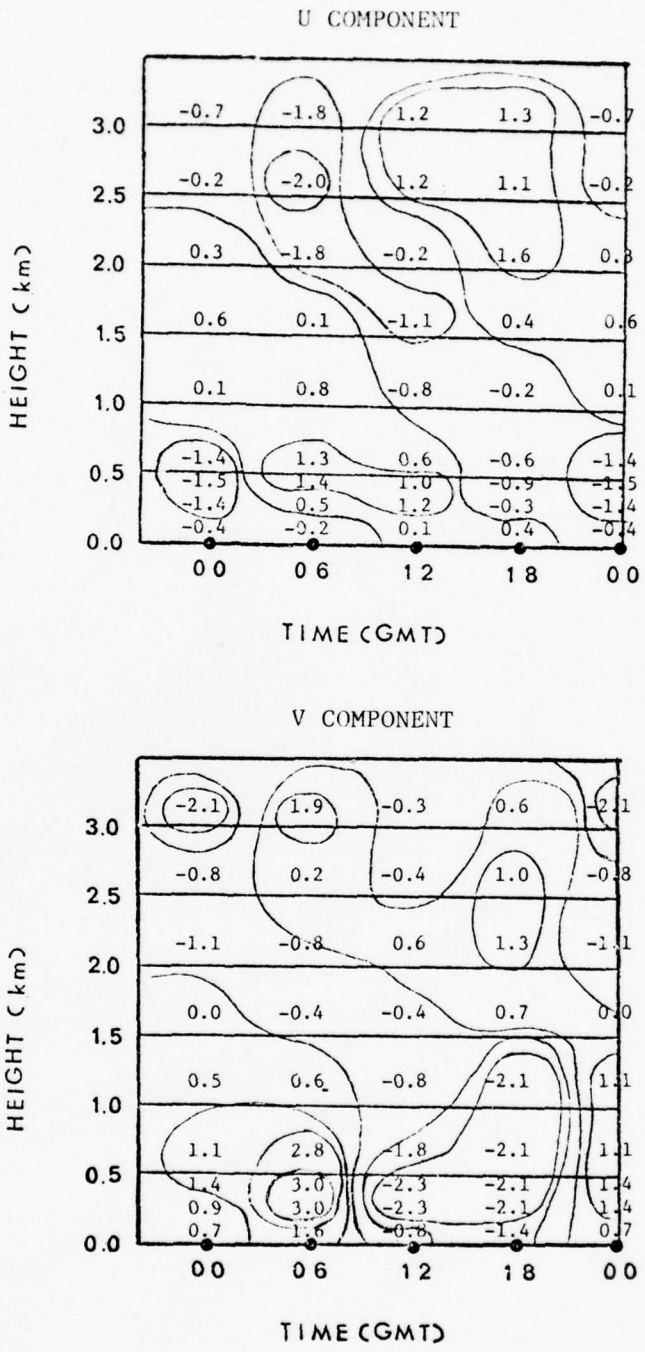

Figure 3.14. Time variation of the deviation in westerly wind from its daily mean at Washington, D. C. Values are in meters per second; times are in GMT.

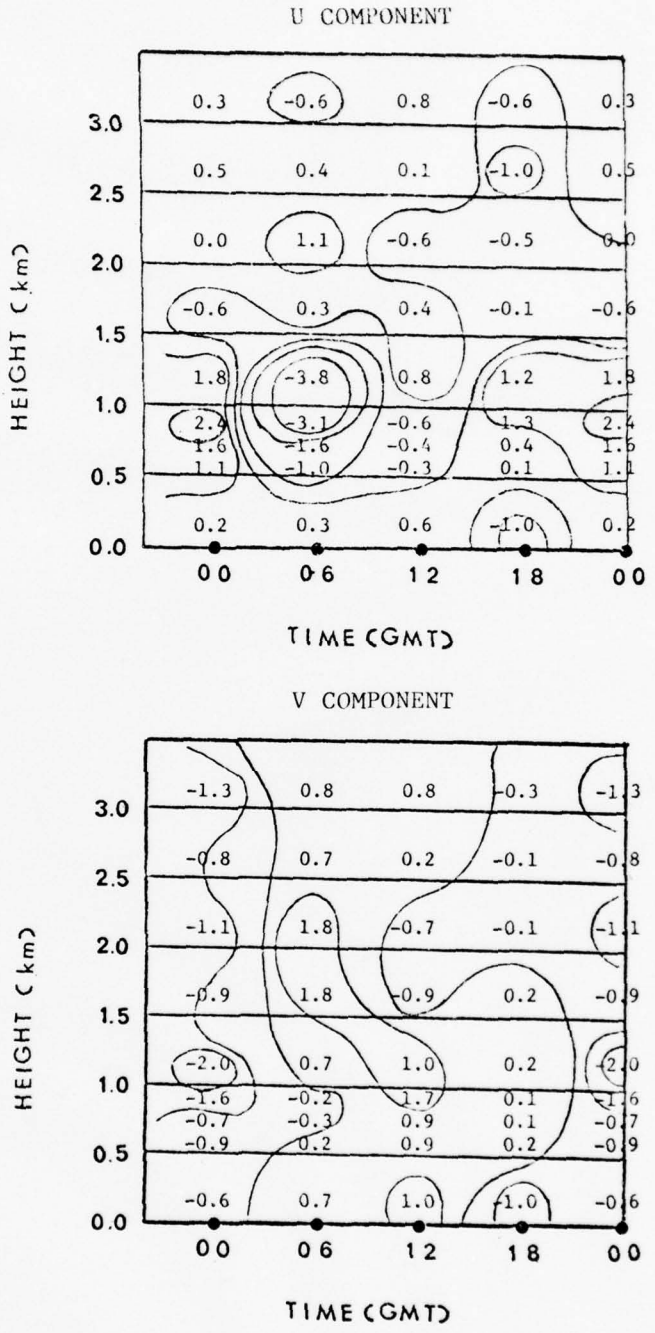

Figure 3.15. Time variation of the deviation in easterly wind from its daily mean at Akron, Ohio. Values are in meters per second; times are in GMT.

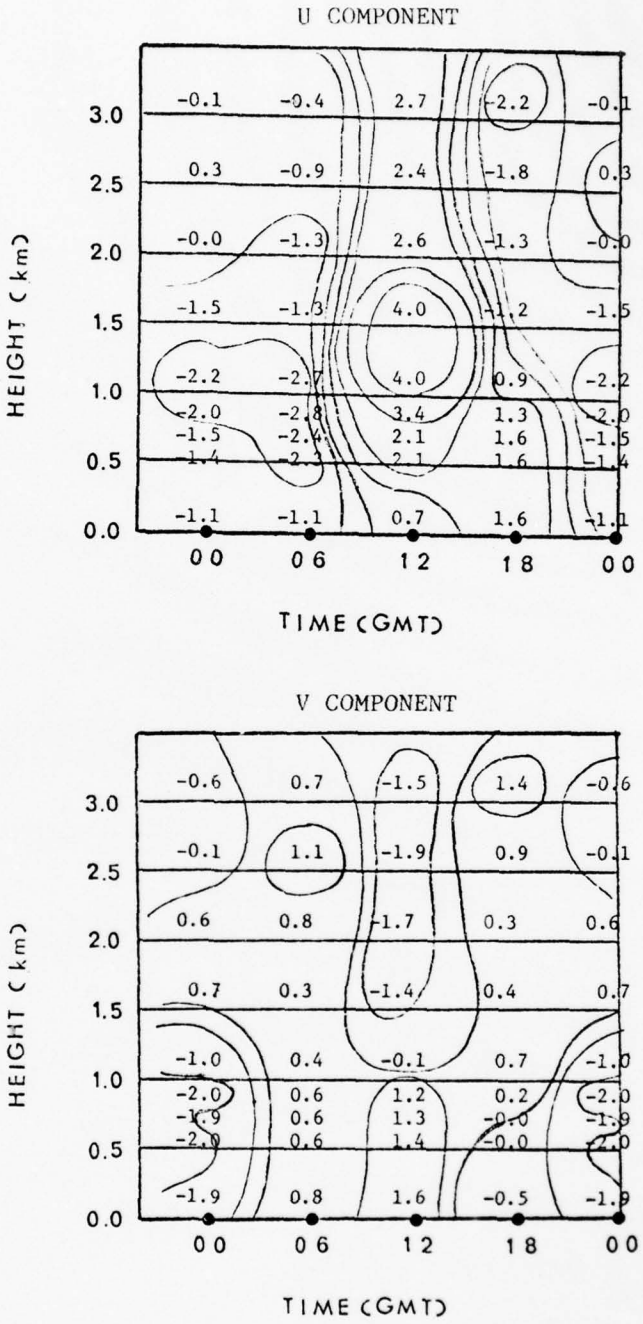

Figure 3.16. Time variation of the deviation in westerly wind from its daily mean at Akron, Ohio. Values are in meters per second; times are in GMT.

rotated 45 degrees to the east to align the V component along the mountain range. The highest terrain between DCA and FNT was west of HAR, which was approximately 1040 m. The wind observations were averaged over the three days of the easterly flow (16-18 July), and the four days of the westerly flow (19-22 July).

Regular Coordinate System

Easterly Flow. At 0600 GMT in the U component (see Figure 3.17), the easterly low-level winds are a maximum over TOL and AKN at 0.5 to 1.0 km MSL. There is very little variation above 1.5 km MSL on the leeward side. In the V component (see Figure 3.18), the low-level winds at DCA and FNT are southerly. There is a southerly component from 1.0 to 2.0 km MSL at AKN and PIT, while above 2.0 km MSL the winds are all northeasterly with a maximum at HAR at 3.0 km MSL.

At 1200 GMT, the flow in the U component (see Figure 3.19) at low-level is about the same as at 0600 GMT, except for lesser magnitudes. The flow at higher levels is approximately the same. The V component at 1200 GMT depicts northerly winds in the low levels except for FNT. The flow at upper levels was approximately the same as the 0600 GMT V cross-section of easterly flow.

At 0000 GMT and 1800 GMT in the U components, the flow in the lower levels was less than at 0600 GMT and 1200 GMT, but the flow was essentially the same direction. There was also little differences between the 0000 GMT and 1800 GMT V cross-sections.

Westerly Flow. At 0600 GMT in the U component (see Figure 3.20), the flow was fairly uniform westerly except for the surface to 0.6 km MSL at AKN and at upper levels over DCA. There was a maximum westerly

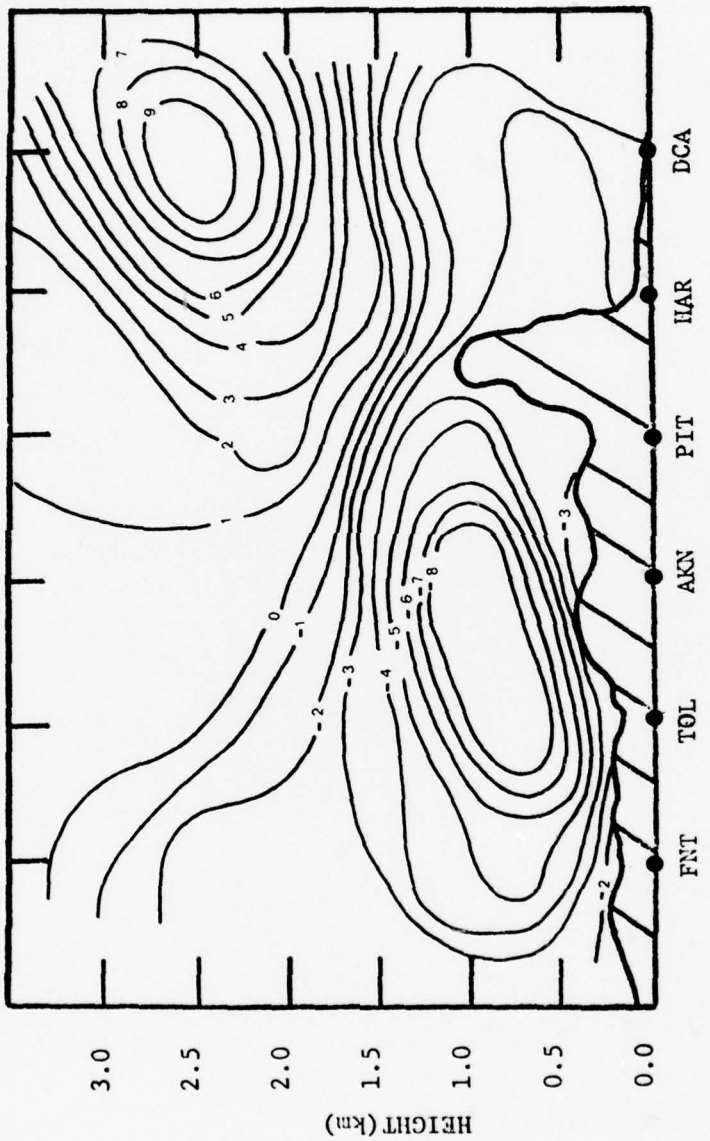

Figure 3.17. Cross-section of 0600 GMT easterly flow (U component) across terrain. Values are meters per second.

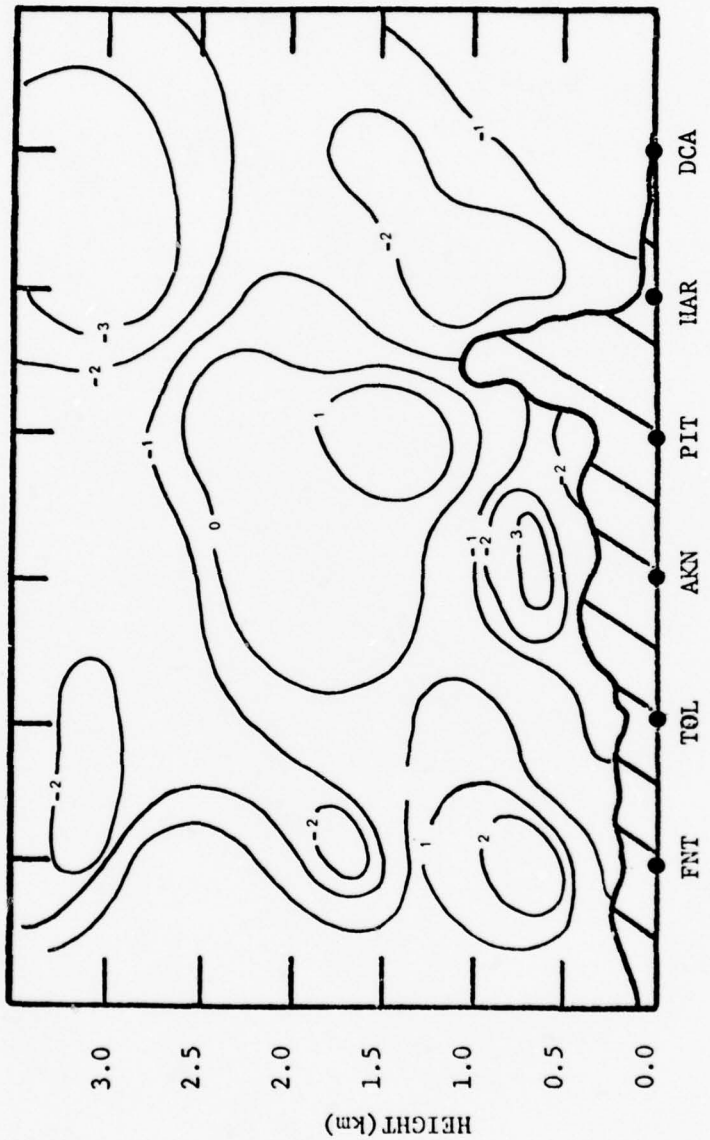

Figure 3.18. Cross-section of 0600 GMT easterly flow (V component) across terrain. Values are meters per second.

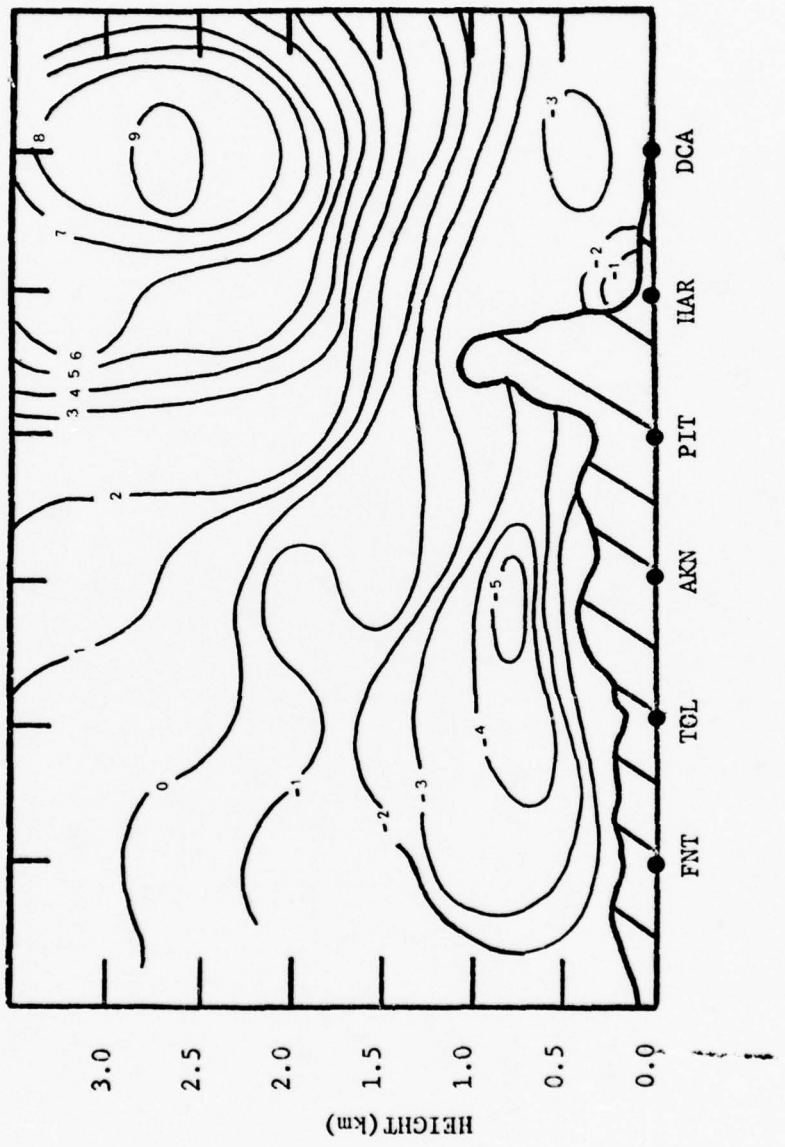

Figure 3.19. Cross-section of 1200 GMT easterly flow (U component) across terrain. Values are meters per second.

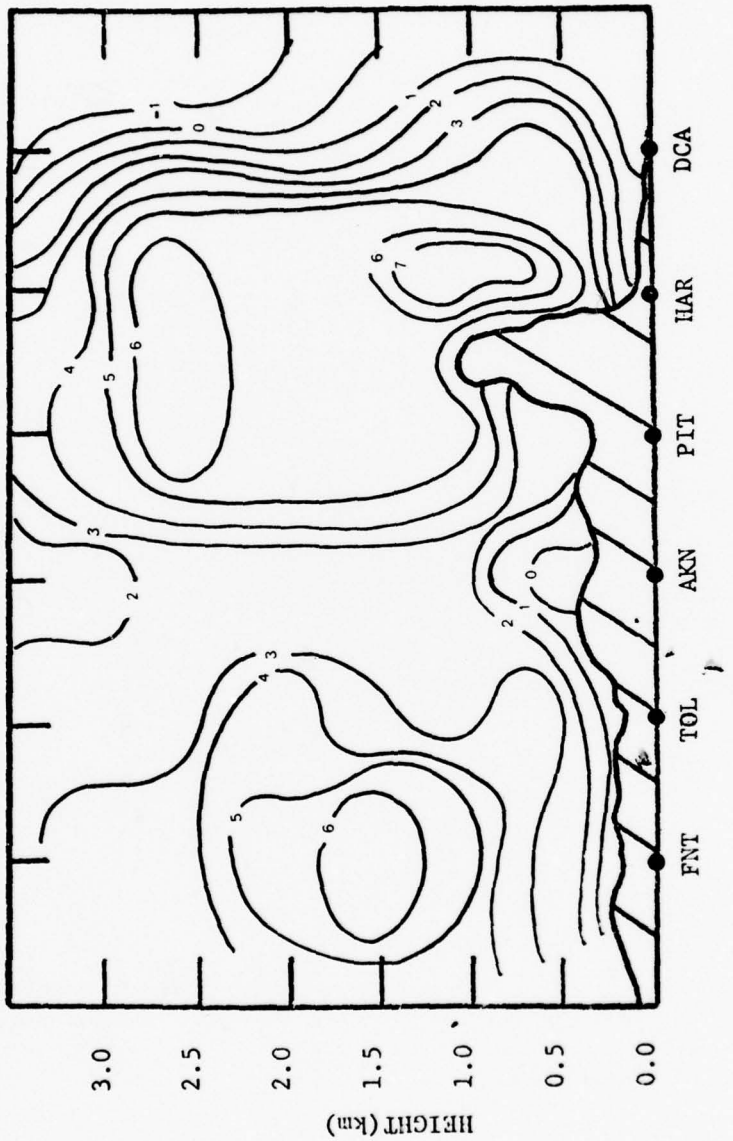

Figure 3.20. Cross-section of 0600 GMT westerly flow (U component) across terrain. Values are meters per second.

at 1.5 km MSL over FNT, and at 0.5 to 2.0 km MSL over HAR. In the V component (see Figure 3.21), the lower level flow was southerly at all stations except for PIT, which was northerly from the surface to 0.5 km MSL. A southerly component of 5 m sec^{-1} was prevalent over DCA at 300 to 600 m MSL. A northerly component of 4 m sec^{-1} occurred at 2.5 km MSL over DCA.

In the U component at 1200 GMT (see Figure 3.22), the flow was uniform westerly from surface to 3.0 km MSL from FNT to DCA, with the wind maximum from 800 to 1500 m MSL, except for HAR and DCA which were 300 to 1000 m MSL. In the V component there was a variation from northerly to southerly winds with little magnitude change except for higher levels.

In the 0000 GMT and 1800 GMT U components, the flow was uniformly westerly, with the maximum magnitude in the upper levels. There was little wind variation in the 0000 GMT and 1800 GMT V components from the 0600 GMT and 1200 GMT components.

Rotated Coordinate Axes

With the axes rotated 45 degrees to the right, the U and V components will be identified as U' and V'.

Easterly Flow. The patterns for all four times of the day in the U' components showed a decrease in the magnitude of the low-level winds, while the upper levels showed a slight increase. The 0600 GMT U' pattern (see Figure 3.23) lower level magnitudes were higher than the other three times.

The 0600 GMT V' pattern (see Figure 3.24) depicts a magnitude increase of 4 to 5 m sec^{-1} in the low levels on the western side of the

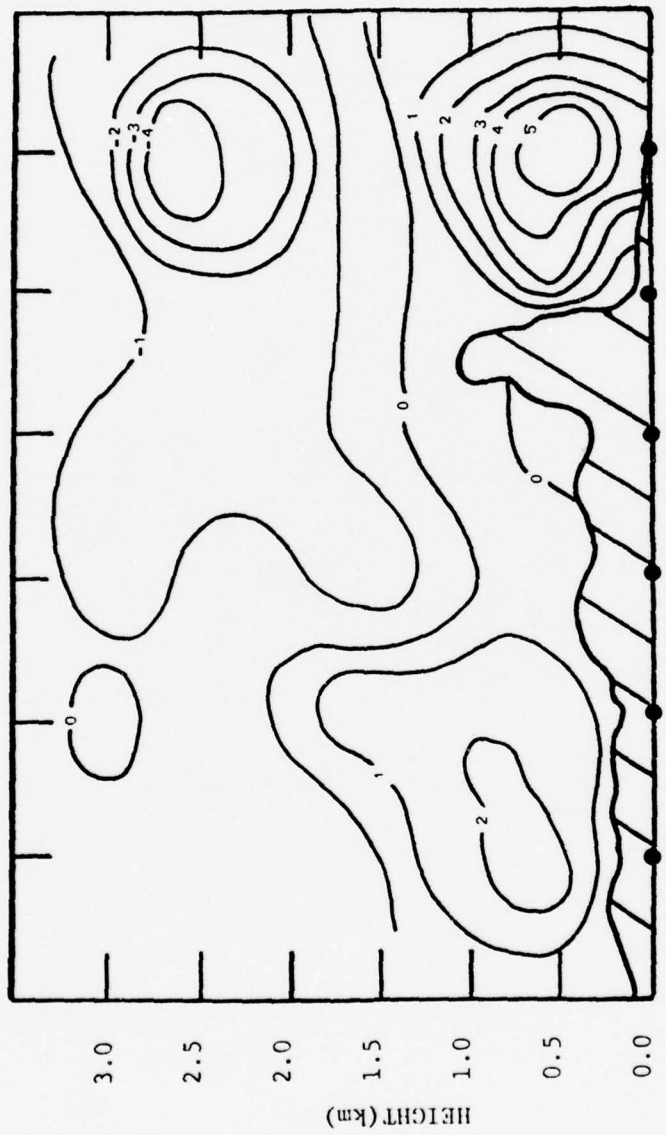

Figure 3.21. Cross-section of 0600 GMT westerly flow (V component) across terrain. Values are meters per second.

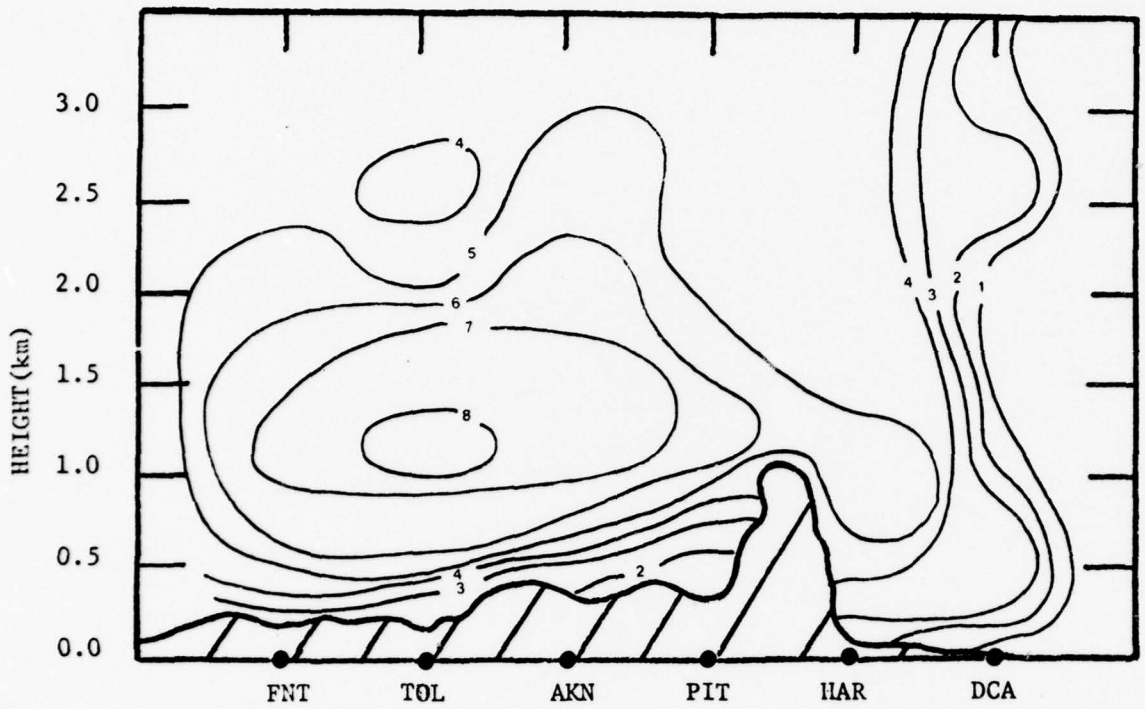

Figure 3.22. Cross-section of 1200 GMT westerly flow (U component) across terrain. Values are meters per second.

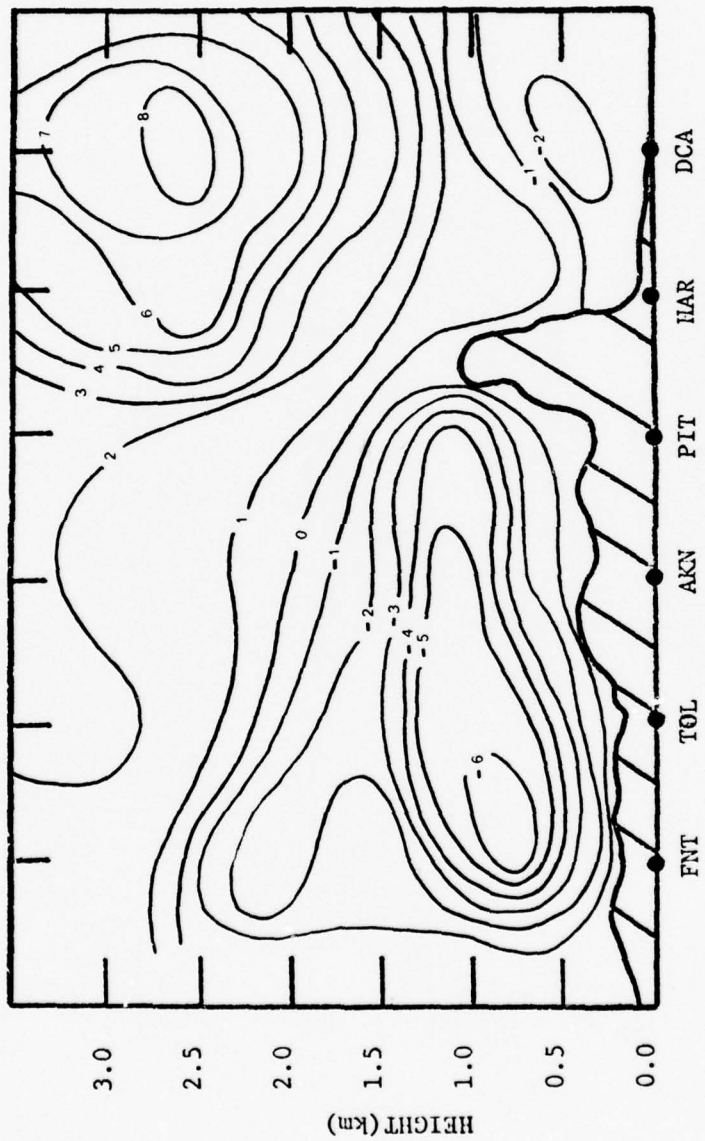

Figure 3.23. Cross-section of 0600 GMT easterly flow (U component) across terrain. Values are meters per second.

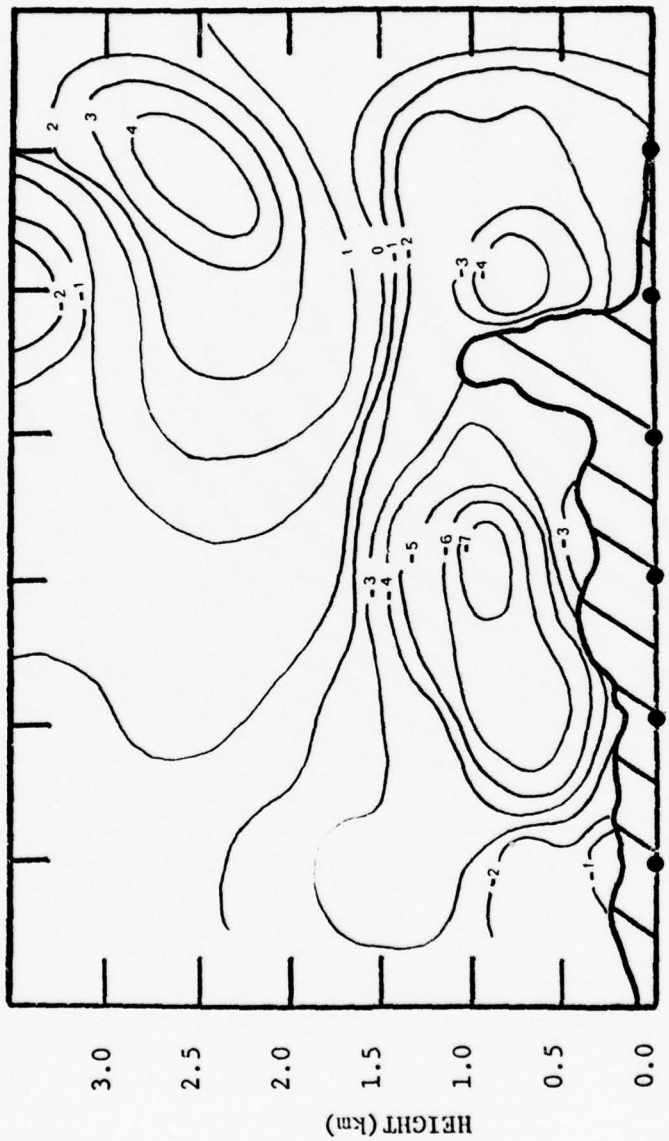

Figure 3.24. Cross-section of 0600 GMT easterly flow (V' component) across terrain. Values are meters per second.

mountain range. In the upper levels over the east coast, the wind components change from the northerly direction in the non-rotated V, to southerly in the rotated V' component. In the 1200 GMT V' component there is little difference from the 1200 GMT V pattern.

The vertical gradient over HAR in the easterly (Figure 3.23) flow is due to a strong upper level flow of westerly winds over a light to moderate wind maximum at the lower levels over the east coast. The low-level jet is very prominent in this flow, as is the upper level maximum winds over the east coast. These upper level winds are due to a trough over the western Atlantic.

Westerly Flow. The U' component patterns of the westerly flow at all four periods of the day is essentially the same as the U components except overall the U' components have lesser magnitudes.

The 1200 GMT V' pattern (see Figure 3.25) is different than the V component in that there is a wind maximum of 4 m sec^{-1} greater in the lower levels over the TOL area. The wind is more parallel to the mountains with the rotated axis. There is little change from the other three time periods in the V' component from the V component except for greater magnitudes.

The low-level jet is a maximum in this easterly flow at 0600 GMT, while in the westerly flow it is a maximum at 1200 GMT. Even though the low-level jet is prominent at 1200 GMT in the west, HAR and DCA have a low-level maximum at approximately 2 m sec^{-1} greater at 0600 GMT. The large gradient on the lee side of the mountains at HAR in the low-level flow at 0600 GMT is partially due to the downslope effect.

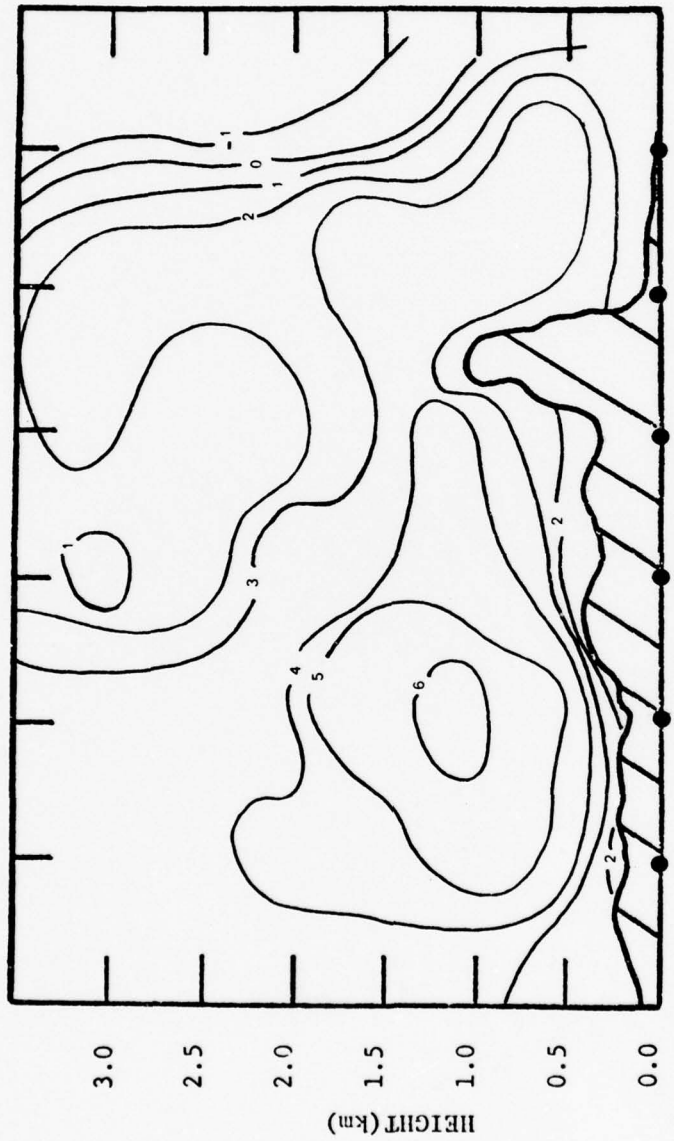

Figure 3.25. Cross-section of 1200 GMT westerly flow (V' component) across terrain. Values are meters per second.

The difference between the rotated and non-rotated axes, is that as the rotated U component decreases in both the easterly and westerly flows, the rotated V component increases in both flows. The upper level jet over the east coast has more of a southeasterly flow, with higher wind speed than the non-rotated axis.

3.3.4. Low-Level Jet

Even though this study is of a recorded air stagnation period (under the influence of a strong high pressure system), the wind profile shows a nocturnal wind maximum in the low levels (500 to 1500 m MSL) in both the easterly and westerly flows. The wind speeds in the stagnation jet does not reach the speed of the low-level jet that occurs over the central plains of the United States (Bonner and Paegle, 1970). Also the low-level jet over the central plains is embedded in a basic current of generally southern flow (Peterson, 1974).

The most significant features of the jet are the diurnal variations of intensity, and the sharp decrease in wind speed above and below the level of maximum wind. A daytime wind distribution with rather small vertical shear gives way to a profile at nigh characterized by very light winds at the surface, 6 to 10 m sec^{-1} at 500-to 1500 m MSL, and less winds (near geostrophic values) within the next higher levels.

Analysis

Height of Low-Level Jet. To analyze the height of the low-level jet, the wind profiles from Section 3.3.1 were evaluated. These wind profiles were days averaged over the three days of the easterly flow, and the four days of the westerly flow.

The easterly profiles showed the maximum wind occurred at 0600 GMT. A comparison of the heights of the jet above mean sea level at above ground are given in Table 2.1.

The significant aspect of this table is the uniformity of the jet height (only 100 m separate the six stations in the above ground levels). An air sample over DCA at 300 m AGL could possibly be transported to the Michigan-Ohio area at the same or approximately the same level across the Appalachians.

The profiles with the westerly flow depicted the maximum low-level jet at 1200 GMT, except for HAR and DCA (on leeward side of mountains) where the maximum wind was still at 0600 GMT. These two stations had a slight increase at 1200 GMT, but not as strong as the wind velocity at 0600 GMT. In the westerly flow, the level of maximum winds occurred at a higher elevation. Table 2.2 depicts the height of the westerly low-level jet.

The level of maximum winds at DCA and HAR depicted in Table 2.2 are for the 1200 GMT flow, even though the low-level winds at the two stations at 0600 GMT are higher in magnitude. The 1200 GMT jet begins to decrease in magnitude in the westerly flow as it crosses the mountain range, contrary to that characteristic of the easterly flow. But the westerly flow of maximum winds also have a uniform height across the area studied, but approximately 400 m higher than the easterly jet. AKN shows a higher level of maximum winds than the other stations, but the difference between 1000 m and 1500 m is 1 m sec^{-1}. There is little difference in magnitude between 500 m and 1000 m at HAR. DCA's level of maximum winds is at a lower altitude than the other five stations, but this could be due to downslope or station elevation.

Table 2.1. Heights of low-level jet in easterly flow in MSL and AGL. (Number in parenthesis is elevations of stations in meters MSL.)

	FNT(233)	TOL(211)	AKN(377)	PIT(373)	HAR(107)	DCA(20)
MSL	533	500	677	673	500	320
AGL	300	289	300	300	393	300

Table 2.2. Heights of low-level jet in westerly flow in MSL and AGL. (Number in parenthesis is elevation of stations in meters MSL.)

	FNT(233)	TOL(211)	AKN(377)	PIT(373)	HAR(107)	DCA(20)
MSL	1000	1000	1500	1000	1000	500
AGL	767	789	1123	627	893	480

Inertial Oscillation Analysis. In analyzing the inertial oscillations of the wind field in our study, the deviation of the wind from its average value was used. The deviation was computed for the particular day at each observation time. Deviations were then averaged over all the days in each series (east and west).

Two stations (AKN and DCA) were selected for study: one on the west side of the mountain range and one on the east side. Instead of using the geostrophic wind which is difficult to determe with confidence, the mean wind over each series was used.

The height of 1.0 km MSL was selected at AKN because this is the level where the surface frictional effect should be minimal and geostrophic flow begins. Sunset at AKN for this time of year was at 0130 GMT (1930L). The period of inertial oscillation was 18 hours and 34 minutes.

In the easterly flow at AKN (leeward side of mountains), the mean wind direction for the three-day period was from 065 degrees. The inertial circle depicts a maximum wind at 0600 to 0700 GMT (see Figure 3.26).

AKN in the westerly flow (windward side of the mountain range) has a mean wind direction for the four-day period from 260 degrees. The inertial circle shows a maximum wind at approximately 1100 to 1200 GMT. (see Figure 3.26).

The 0.5 km MSL was selected at DCA, because at 1.0 km MSL the wind speed is decreasing (see Figure 3.27). Also this height above DCA is where the surface frictional effects are diminishing, as the station elevation is 20 m. Sunset at DCA was at 0120 GMT (1920L), and the period of inertial oscillation was 19 hours and 16 minutes.

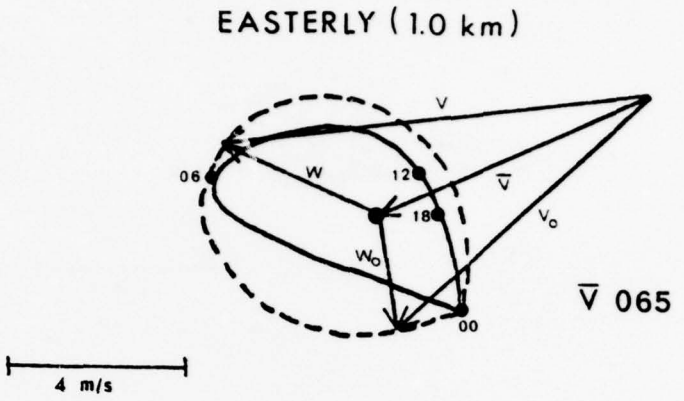

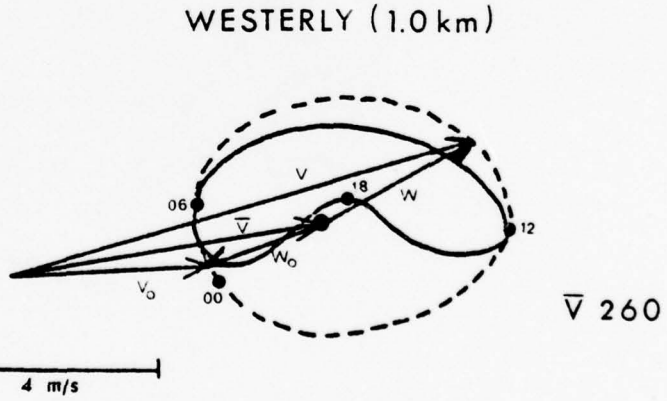

Figure 3.26. Hodographs of the wind variation at AKN in the easterly and westerly flow. Heights are MSL; times are GMT.

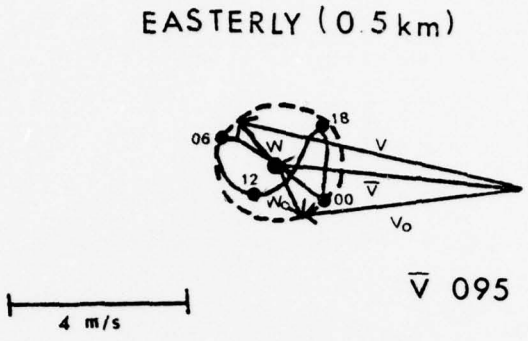

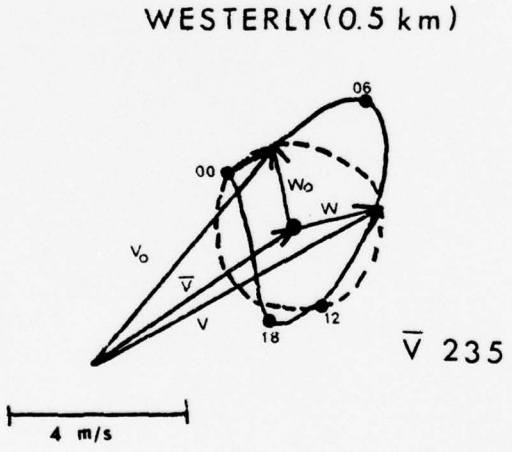

Figure 3.27. Hodographs of the wind variation at DCA in the easterly and westerly flow. Heights are MSL; times are GMT.

In the easterly flow the mean wind for the three-day period was from 095 degrees. Figure 3.27 shows the time of maximum wind at approximately 0600 to 0700 GMT, which is about one-quarter of the pendulum day, or about 9 hours and 38 minutes after sunset.

In the westerly flow the mean wind for the four-day period was from 235 degrees. The inertial circle depicts a maximum wind at 0600 to 0800 GMT (see Figure 3.27).

These results agree with Buajitti (1957) that drainage is not the cause of observed variations, in view of the phase of the variations. Heating and cooling of the lower layer above a sloping surface results in a downhill force at night, and an uphill force during the day. Drainage may have some effect near the surface, but not at the level of the low-level jet.

The role of thermal forcing in the diurnal oscillation does have an effect on the variation of the wind above mountainous terrain. According to Hoxit (1973), diurnal changes in the lapse rate for the lowest 2 km under basically clear conditions tends to force an inertial boundary layer above 200 to 300 m shortly after sunset and to give an order of magnitude variation in the depth of the momentum boundary layer.

It is therefore concluded that the low-level jet examined in this air stagnation period can be explained by an inertial type oscillation driven by the diurnal variation of the frictional force aided by thermal forcing.

3.3.5. Analysis of Diurnal Oscillations across Mountainous Terrain

The diurnal oscillation hodograms were drawn across the north central Appalachians for the six stations in this study. The levels of 0.5 and 1.0 m MSL were selected as they were most representative of the oscillations. The hodographs were drawn for the easterly and westerly flows. The deviations of the averaged wind speeds from their means were used in drawing these hodograms.

As this study was conducted for an air stagnation period, the lower atmosphere should be fairly stable. The easterly flow should be more stable than the westerly flow, as the westerly flow begins to show some of the characteristics of the next weather system. Holton (1967) stated that positive stability reduces the amplitude of the oscillation, decreases the height of maximum amplitude, and increases the ellipticity of the hodographs. Another factor that affects the shape of hodographs is the presence of the low-level wind maximum. This wind maximum causes the shape of the hodograph to be more elongated.

In the easterly flow at 0.5 km MSL (see Figure 3.28) the oscillations were larger at HAR, TOL, and FNT than they were at PIT, AKN, and DCA. This is due to the height of the low-level jet, located at 300 m AGL. FNT, TOL, and HAR at 0.5 km were closer to the low-level jet than were the other three stations (see station elevations in Table 2.1). The elongation of the hodographs is more pronounced at stations where the altitude employed is near that of the low-level jet.

At 0.5 km MSL in the westerly flow (see Figure 3.29), the oscillations are larger than in the easterly flow at all the stations except for HAR. The large oscillations are influenced somewhat by the surface frictional effects as this level is well below the low-level jet from the west except for DCA.

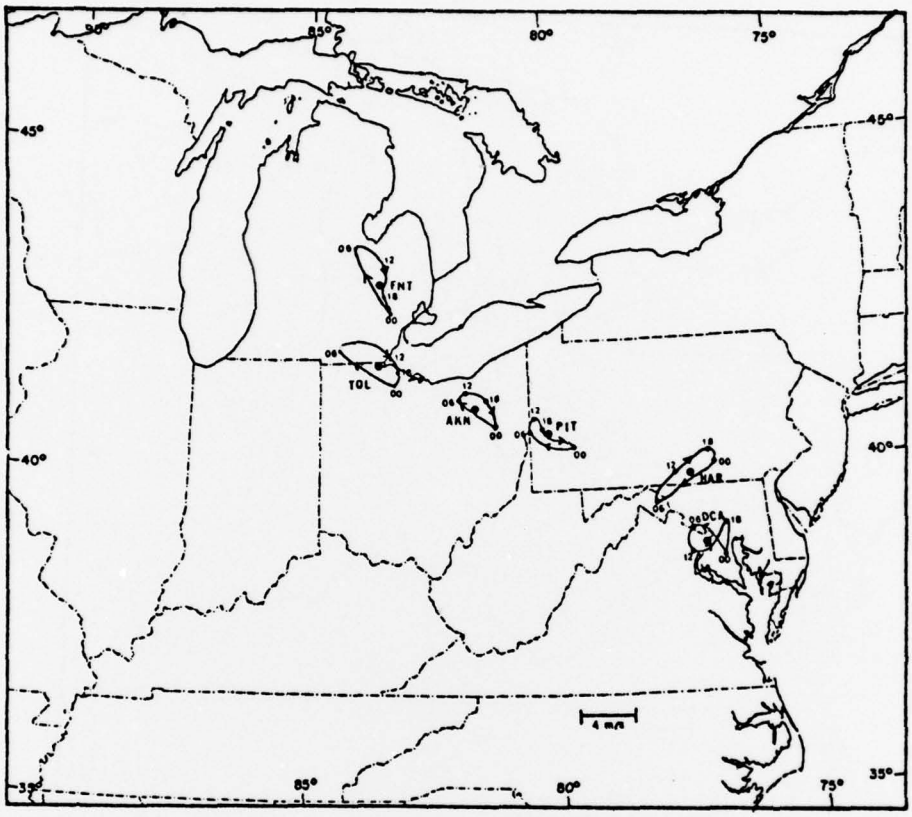

Figure 3.28. Hodographs of the wind variation in easterly flow at 0.5 km (MSL). Times are GMT.

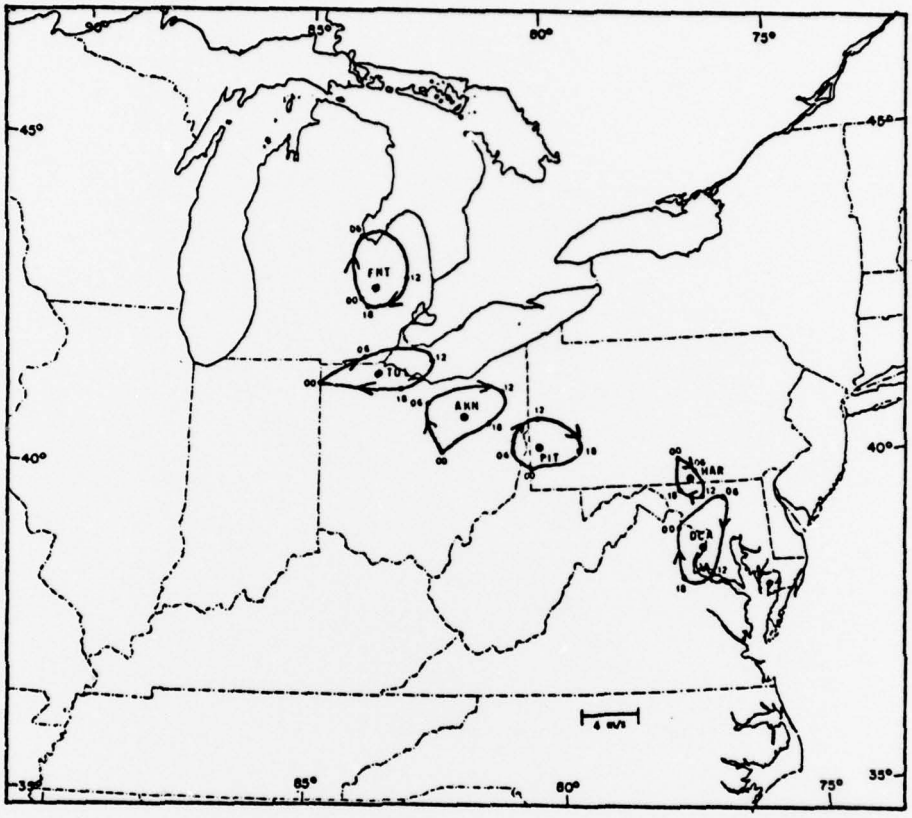

Figure 3.29. Hodographs of the wind variation in westerly flow at 0.5 km (MSL). Times are GMT.

The easterly flow at 1.0 km (see Figure 3.30) depicts more elongated ellipses at stations on the leeward side of the mountain range, while HAR and DCA are more circular. The flow is well above the low-level jet at 1.0 km MSL. The oscillations follow the pressure patterns fairly well until they attain the 0600 GMT point (where wind is a maximum). All of the stations have anticyclonic flow except for FNT.

In the westerly flow at 1.0 km MSL (see Figure 3.31), the stations on the windward side have elongated ellipses. On the windward side this is about the level of the westerly low-level jet. The stations on the leeward side depict hardly any effect of the low-level jet, as they are above the level of frictional influences and appear to be in the layer of pure geostrophic flow.

In a study by Kao, Paegle and Normington (1974), they stated that below mountaintops, on the windward side, mountains tend to partially divert the component of the mean motion normal to the mountains to that parallel to the mountains. This flow is evident at the 1.0 km MSL level at HAR and DCA in the easterly flow, and at PIT in the westerly flow. It is not as evident in the 0.5 km MSL flow at HAR and DCA in the easterly flow, but there is some of this effect. In the westerly flow PIT and AKN are examples of this type.

Applying Holton's positive stability theory to this study, we can see that the amplitudes of the hodographs are reduced in the easterly flow more so than in the westerly flow. This indicates that stratification can contribute significantly to the amplitude of the diurnal wind oscillations over sloping terrain.

This analysis aids in reinforcing the postulation of the low-level wind maximum across mountainous terrain being explained by the

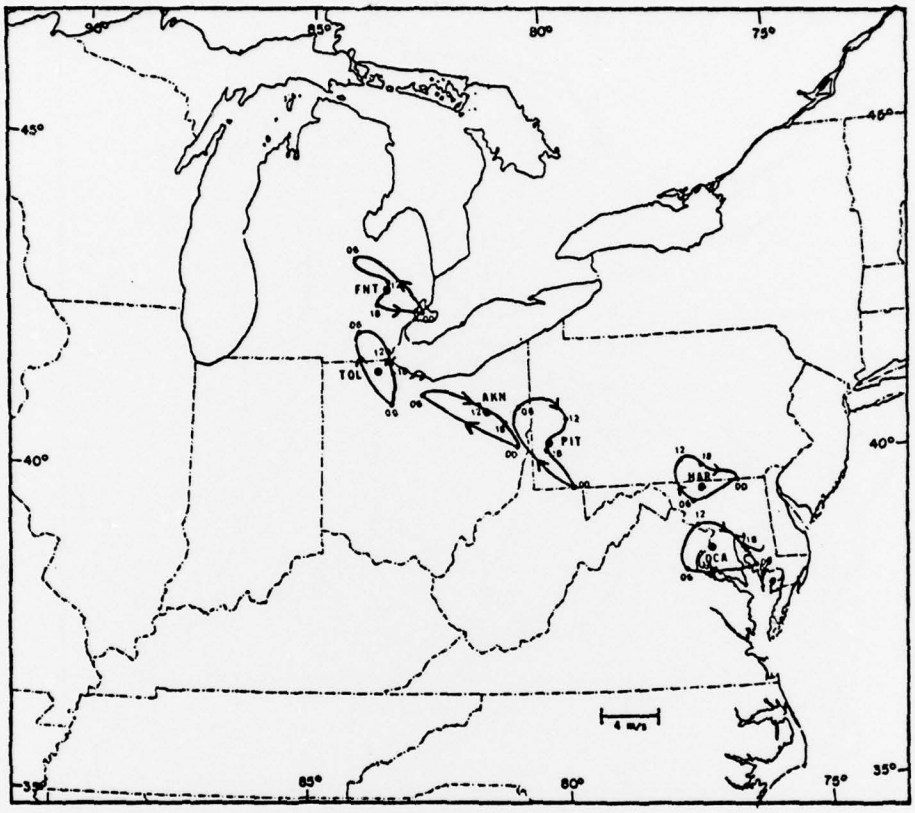

Figure 3.30. Hodographs of the wind variation in easterly flow at 1.0 km (MSL). Times are GMT.

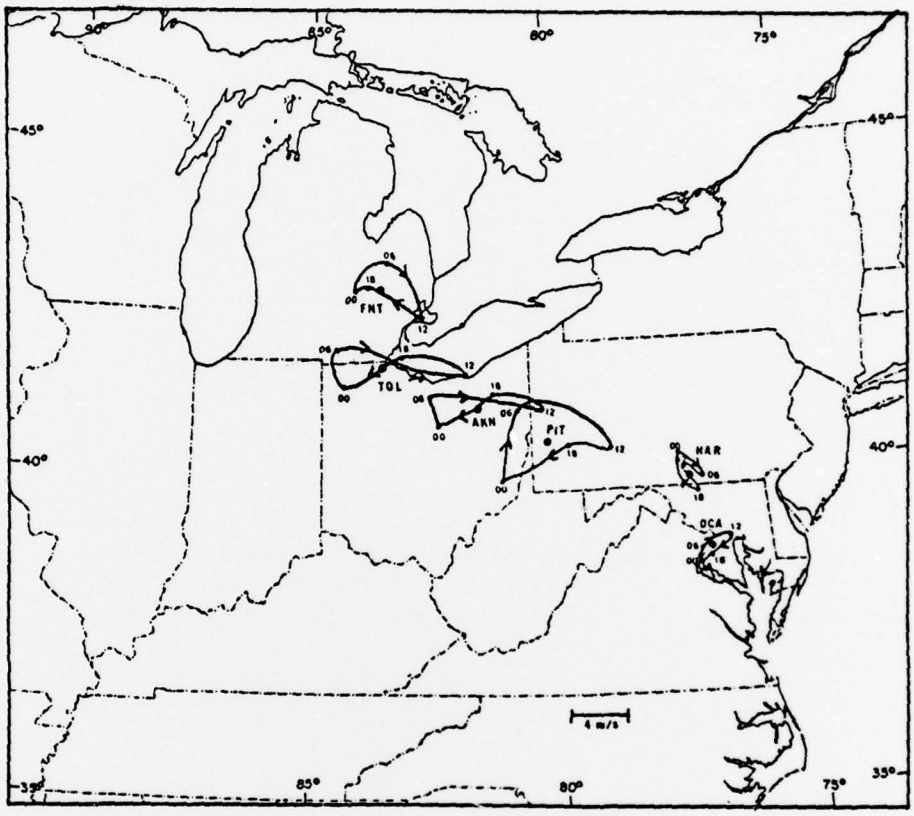

Figure 3.31. Hodographs of the wind variation in westerly flow at 1.0 km (MSL). Times are GMT.

inertial oscillation driven by the diurnal variation of the frictional forces aided by thermal forcing.

4. AIR POLLUTANTS TRANSPORT POTENTIAL

Discharge of pollutants to the air during meteorological conditions conducive to their congestion could be reduced or eliminated for many sources of pollutions provided adequate and dependable warning of the conditions were given. When conditions are favorable for rapid dispersion and diffusion of contaminants, higher rates of discharge are possible without creating undesirable effects. Occasionally meteorological conditions develop which inhibit dispersion of airborne wastes for extended periods. Forecasts of the latter conditions, coupled with measurements of air quality, could provide a basis for pollution control.

A forecast of unfavorable atmospheric conditions would alert interested parties to take precautionary measures. Measurement of local air contaminants could then be initiated to monitor the air quality. If these measurements attained prescribed values, and the forecast indicated that meteorological elements necessary to the accumulation of contaminants were expected to persist, the appropriate steps could be taken to reduce or eliminate the emission of pollutants until the measurements and the forecasts show that normal activity could be resumed (Niemeyer, 1960).

This study of a stagnation period could be used as a guide in forecasting the rapid dispersion of pollutants at night. During the daylight hours, comtaminants are entrained into the atmosphere and vertically mixed. Even though the area is under the influence of a high pressure system, there is still some vertical mixing occurring, especially over mountainous terrain. During the night the nocturnal inversion develops and and traps pollutants below the inversion, but the contaminants above the inversion are free to be transported with the wind flow.

Theoretically, in the easterly flow, pollutants above 300-500 m AGL can be ferried rapidly from the eastern coastal areas to the western Pennsylvania and Ohio areas at approximately 0600 GMT. In the westerly flow the contaminants could be transported most rapidly at 1200 GMT from the Ohio and western Pennsylvania areas to the eastern seaboard at 500-1000 m AGL.

Therefore, interested parties should be concerned, when this type of air stagnation period occurs, with the easterly flow across the mountains at 0600 GMT, and the westerly flow at 1200 GMT. These are the approximate times of possibly maximum transport as shown in this study.

5. CONCLUSION

The wind profiles examined in this air stagnation period have shown that there is a low-level jet across mountainous terrain during an air stagnation period. The profiles also show that the boundary layer winds decrease significantly above the level of maximum winds and remain fairly uniform up to 3.0 km.

Observed winds at Washington, D. C. depict a diurnal oscillation with an amplitude of 3-4 m sec^{-1} at 1.0-1.5 km above the ground in the easterly and westerly flows. At Akron, Ohio, a diurnal oscillation with an amplitude of 4.0 m sec^{-1} occurs at levels of 0.6-1.1 km above the ground.

The analysis of the flow over the terrain has shown that the low-level jet is at different altitudes depending on the wind direction across the mountains. The time of the day is also a factor in the occurrence of the low-level jet, as the easterly maximum low-level wind flow occurs at 0600 GMT, and in the westerly flow it occurs at 1200 GMT. The flow across the terrain has also shown that with rotated coordinate axes, the wind decreases in magnitude in the U component in both the easterly and westerly flows.

This study of inertial oscillation above the terrain indicates that below the mountain top, on the windward side, the mountains tend partially to divert the component of the mean motion normal to the mountains to that parallel to the mountains. It also aids in explaining the wind maximum in the low-levels by an inertial type oscillation driven by the diurnal variation of the frictional force aided by thermal effects.

An extensive analysis of the diurnal winds across the north central Appalachian Mountains has shown that there is a low-level jet across mountainous terrain during an air stagnation period. This jet is similar to the low-level jet over the Central Plains, but is reduced in magnitude. This low-level maximum of winds can be effective in transporting and dispersing of air pollutants across mountains.

6. LIST OF REFERENCES

Blackadar, A. K., 1957: Boundary Layer Wind Maxima and their Significance for the Growth of Nocturnal Inversions. Bulletin American Meteorology Society, Vol. 38(5), pp. 283-290.

Blackadar, A. K., and K. Buajitti, 1957: Theoretical Studies of Diurnal Wind Variation in the Planetary Boundary Layer. Quarterly Journal Royal Meteorological Society, Vol. 83, pp. 486-500.

Bonner, W. D., and J. Paegle, 1970: Diurnal Variation in Boundary Layer Winds over the South-Central United States in Summer. Monthly Weather Review, Vol. 19(2), pp. 199-205.

Hering, W. S., and Thomas R. Borden, 1962: Diurnal Variations in the Summer Wind Field over the Central United States. Journal Atmospheric Science, Vol. 19(1), pp. 81-86.

Hess, S. L., 1959: Introduction to Theoretical Meteorology. Holt, Rinehart and Winston, Inc., N. Y. pp. 189-196.

Holton, J. R., 1967: Diurnal Boundary Layer Wind Oscillation above Sloping Terrain. Tellus, Vol. 19(2), pp. 199-205.

Hoxit, L. K., 1973: Variability of Planetary Boundary Layer Winds. CSU-ATSP-199, Contract/Grant No. NSFGA-32589X1. Colerado State University, pp. 1-157.

Kao, S. K., J. N. Paegle and W. E. Normington, 1974: Mountain Effect on the Motion in the Atmospheres Boundary Layer. Boundary Layer Meteorology, Vol. 7, pp. 501-512.

Korshover, J., 1976: Climatology of Stagnating Anticyclones East of the Rocky Mountains, 1936-1975. NOAA Tech. Mem. ERL ARL-55, U. S. Department of Commerce, 27 pp.

Lettau, H. H., 1967: Small to Large-Scale Features of Boundary Layer Structure over Mountain Slopes. Proceedings of the Symposium on on Mountain Meteorology, E. R. Reiter and J. L. Rasmussen, eds., Atmosphere Science Paper No. 122, Department Atmosphere Science, Colorado State University, Ft. Collins, Colorado, pp. 1-74.

Niemeyer, L. E., 1960: Forecasting Air Pollution Potential. Monthly Weather Review, Vol. 88(3), pp. 88-96.

Peterson, R. E., 1974: A Model of the Low-Level Jet with Variable Eddy Viscosity. Tellus, Vol. 26, pp. 560-563.

LIST OF REFERENCES (Continued)

United States Environmental Protection Agency, 1975: Position Paper on Regulation of Atmospheric Sulfates. Report No. EPA-450/2-75-007, Strategies and Air Standards Division, Research Triangle Park, N. C.

Wexler, H., 1961: A Boundary Layer Interpretation of the Low-level Jet. Tellus, Vol. 13, pp. 368-377.